Oceanic fingerprints of continental and glacial terrestrial runoff in Inuit Nunangat, the Canadian Arctic Archipelago

Birgit Rogalla[1], Susan E. Allen[1], Manuel Colombo[2], Paul G. Myers[3], and Kristin J. Orians[1]

[1]University of British Columbia
[2]Woods Hole Oceanographic Institution
[3]University of Alberta

January 30, 2023

Abstract

Arctic river discharge and terrestrial runoff are observed, and forecasted to continue, changing dramatically due to climate change. Rising temperatures and an acceleration of the hydrological cycle are increasing discharge, causing permafrost thaw, glacial melt, and a shift to a groundwater-dominated system. These changes are funnelled to coastal regions of the Arctic Ocean where the implications for the distributions of nutrients and biogeochemical components are unclear. In this study, we investigate the impact of terrestrial runoff on marine biogeochemistry in Inuit Nunangat (the Canadian Arctic Archipelago) — a key pathway for transport and modification of waters from the Arctic Ocean to the North Atlantic — using sensitivity experiments from 2002-2020 with an ocean model of manganese (Mn). The micronutrient Mn traces terrestrial runoff and the modification of geochemical constituents of runoff during transit. The heterogeneity in Arctic river composition creates distinct oceanic fingerprints of influence: continental runoff influences the southwestern Archipelago, glacial runoff dominates the northeast, and their influence overlaps in central Parry Channel. Glacial runoff carries micronutrients southward from Nares Strait in the late summer and may help support long phytoplankton blooms in the Pikialasorsuaq polynya. Enhanced glacial runoff may increase micronutrients delivered downstream to Baffin Bay, accounting for up to 18% of Mn fluxes seasonally and 6% annually. These findings highlight how climate induced changes to terrestrial runoff impact the geochemical composition of the marine environment, and will help to predict the extent of these impacts as a result of ongoing alterations of the Arctic hydrological cycle.

Oceanic fingerprints of continental and glacial terrestrial runoff in Inuit Nunangat, the Canadian Arctic Archipelago

B. Rogalla[1], S. E. Allen[1], M. Colombo[1], P. G. Myers[2], K. J. Orians[1]

[1]Department of Earth, Ocean, and Atmospheric Sciences, University of British Columbia, Vancouver, British Columbia V6T1Z4, Canada

[2]Department of Earth and Atmospheric Sciences, University of Alberta, 1-26 ESB, Edmonton, Alberta T6G2E3, Canada

Key Points:

- The heterogeneity in Arctic river types creates distinct patterns of influence in the Canadian Arctic Archipelago coastal ocean
- Glacial runoff from Nares Strait supplies micronutrients such as Mn to the Pikialasorsuaq or North Open Water polynya
- Changes in glacial runoff composition in the Canadian Arctic Archipelago and northwestern Greenland are conveyed downstream into Baffin Bay

Corresponding author: Birgit Rogalla, brogalla@eoas.ubc.ca

Abstract

Arctic river discharge and terrestrial runoff are observed, and forecasted to continue, changing dramatically due to climate change. Rising temperatures and an acceleration of the hydrological cycle are increasing discharge, causing permafrost thaw, glacial melt, and a shift to a groundwater-dominated system. These changes are funnelled to coastal regions of the Arctic Ocean where the implications for the distributions of nutrients and biogeochemical components are unclear. In this study, we investigate the impact of terrestrial runoff on marine biogeochemistry in Inuit Nunangat (the Canadian Arctic Archipelago) — a key pathway for transport and modification of waters from the Arctic Ocean to the North Atlantic — using sensitivity experiments from 2002-2020 with an ocean model of manganese (Mn). The micronutrient Mn traces terrestrial runoff and the modification of geochemical constituents of runoff during transit. The heterogeneity in Arctic river composition creates distinct oceanic fingerprints of influence: continental runoff influences the southwestern Archipelago, glacial runoff dominates the northeast, and their influence overlaps in central Parry Channel. Glacial runoff carries micronutrients southward from Nares Strait in the late summer and may help support long phytoplankton blooms in the Pikialasorsuaq polynya. Enhanced glacial runoff may increase micronutrients delivered downstream to Baffin Bay, accounting for up to 18% of Mn fluxes seasonally and 6% annually. These findings highlight how climate induced changes to terrestrial runoff impact the geochemical composition of the marine environment, and will help to predict the extent of these impacts as a result of ongoing alterations of the Arctic hydrological cycle.

Plain Language Summary

In the Arctic, climate change is expected to increase river flow and alter the composition of river water through permafrost thaw and glacial melt. Many rivers and land areas drain to the coastal areas of the Arctic Ocean; the impact of changes to the nutrients in the river water to these regions are unclear. In this study, we focus on Inuit Nunangat (the Canadian Arctic Archipelago) — a shallow series of channels that connects the Arctic Ocean to the North Atlantic — and look at where in the ocean the material in the river water ends up and how much of the material travels downstream. We use experiments with an ocean model from 2002-2020 and track an element found in river water: manganese (Mn), which is also an important nutrient in the ocean. While con-

tinental rivers mainly influence the southwestern Archipelago, glaciers influence the northeastern Archipelago and supply nutrients to Pikialasorsuaq, one of the Arctic's most biologically active areas. Glaciers can also contribute up to 18% to Mn transported downstream of Nares Strait seasonally and 6% yearly. Our findings highlight how climate related changes in the composition of river water impact Inuit Nunangat and how these changes can funnel downstream.

1 Introduction

All components of the Arctic freshwater system are experiencing shifts as a result of human-induced climate change (Serreze et al., 2006; White et al., 2007). Almost half of the freshwater contributed annually to the Arctic Ocean originates from rivers (Haine et al., 2015) and these rivers are fed by catchment basins that stretch far south, transferring lower latitude changes to the high latitudes. River runoff integrates large-scale climatic changes over these basins and transmits them to the continental shelves and Arctic Ocean where the river runoff delivers freshwater, heat, sediments, and nutrients (Holmes et al., 2012). Observed and forecasted changes to Arctic rivers include enhanced discharge (Peterson et al., 2002; McClelland et al., 2006; Feng et al., 2021), a shift towards a groundwater-dominated system (Walvoord & Striegl, 2007), increased sediment and organic carbon supply from permafrost thaw (Spencer et al., 2015; Aiken et al., 2014), glacial melt (Bhatia et al., 2013), and altered river geochemistry (Frey & McClelland, 2009). These changes will lead to an altered biogeochemical signature in rivers throughout the Arctic (Frey & McClelland, 2009). The long-term effects of these changes on ocean biogeochemical cycles, circulation patterns, and primary productivity are far from understood, but evidence suggests that they will have substantial impacts both in the Arctic Ocean (Wrona et al., 2016; Prowse et al., 2015) and downstream in subpolar seas (Greene & Pershing, 2007).

Inuit Nunangat, or the Canadian Arctic Archipelago (CAA), is characterized by an abundance of rivers, many shallow channels, and extensive coastlines which modify the biogeochemical properties of water as it transits from the Arctic Ocean to Baffin Bay and the north Atlantic Ocean (Rogalla et al., 2022; in review; Colombo et al., 2021) — these properties make it an ideal place to study the influence of rivers on the Arctic marine environment. The CAA is also highly productive and home to the northern hemisphere's largest polynya: the Pikialasorsuaq or North Water polynya. A few large rivers

such as the Mackenzie River, drain the North American continent, alongside many smaller rivers and streams that flow from the continent and islands into the channels of the CAA (Prowse & Flegg, 2000). These extensive freshwater systems form a recurrent feature along coastlines termed the Riverine Coastal Domain (RCD), which connects terrestrial and marine ecosystems (Carmack et al., 2015). Differences in seasonal hydrology, bedrock geology, catchment basin scales, and landscape processes drive the heterogeneity of the geochemical characteristics of rivers in the CAA (Alkire et al., 2017; Colombo et al., 2019; Brown, Williams, et al., 2020; Grenier et al., 2022). The majority of the CAA also has some form of continuous or discontinuous permafrost (Frey & McClelland, 2009) and glaciers covering northeastern regions including Ellesmere Island and Baffin Island. As a result of the predicted increased terrestrial runoff in a future climate, the RCD may become more prominent and its composition will likely be altered (Carmack et al., 2015).

Over the last few decades, research efforts into the Arctic freshwater system have expanded (Bring et al., 2016) using a range of methods: direct and remotely sensed observations, modelling studies, and conceptual frameworks. Feng et al. (2021) combined hydrologic modelling and remote sensing to produce an overview of pan-Arctic river runoff and Stadnyk et al. (2020) improved hydrological modelling of runoff into Hudson Bay. Long time series of river discharge and composition measurements exist for the "big-6" Arctic rivers (the Mackenzie, Yukon, Yenisey, Lena, Laptev, and Ob) from the Arctic Great Rivers Observatory (Arctic-GRO) and PARTNERS projects (McClelland et al., 2015). Other recent studies have expanded on this information by studying the composition of runoff from smaller rivers in the Canadian Arctic Archipelago (Colombo et al., 2019; Brown, Williams, et al., 2020). In the coastal oceans, the small size of the band of river influence (generally less than 10 km) makes observations sparse (Carmack et al., 2015). Climate models have focused on predicting hydrological changes to rivers (Nijssen et al., 2001) and the impact of freshwater on the physical dynamics of the ocean (Lique et al., 2016). Recent improvements in the resolution of these models allow for more detailed experiments of the role of runoff on coastal ocean chemistry (Tank et al., 2012). Lagrangian modelling has been used to identify meltwater pathways from the Greenland Ice Sheet into Baffin Bay (Gillard et al., 2016). Remotely sensed chromophoric dissolved organic matter (CDOM) has also been demonstrated as a helpful tool for tracing riverine influence in the Arctic Ocean, however satellites observe only the surface signatures (Fichot et al., 2013) and are limited by sea ice cover. Several conceptual studies and syn-

theses (Brown, Williams, et al., 2020; McClelland et al., 2012; Carmack et al., 2015) have established frameworks within which to understand anticipated and observed changes to rivers in the ocean context. However, despite all this progress, we lack quantification of the extent to which the marine environment is linked to terrestrial runoff and how environmental changes will alter this important freshwater input.

The impact of geochemical constituents in terrestrial runoff on the marine environment is not only a function of ocean dynamics, but also the chemical and biological processes that alter the composition of water during transit in the ocean. While model experiments tracing runoff with "dye" or measurements of the dissolved oxygen isotope ratio are able to identify terrestrial freshwater or meteoric water presence, these approaches do not account for the modification (change of oxidation state, removal) of geochemical constituents over time. Manganese (Mn) is a trace element and essential micronutrient (Sunda, 2012) with advantageous properties for tracing terrestrial runoff that incorporates information related to oxidation-reduction and removal. Mn has a scavenged-type vertical distribution with maximum concentrations near sources and low background concentrations; this contrast allows it to be used as a tracer of inputs such as terrestrial runoff (Landing & Bruland, 1980; Middag et al., 2011). Oxidation removes dissolved Mn on the time scale of weeks to months (Rogalla et al., 2022; in review; Van Hulten et al., 2017) and as it undergoes reversible scavenging and sinking, it remains in the ocean surface up to a few years (Landing & Bruland, 1987; Shiller, 1997; Jickells, 1999; Kadko et al., 2019). This timescale of Mn presence in the ocean is conducive to studying the transport of geochemical constituents. The distribution of Mn also informs runoff impacts on other lithogenic-derived elements in the Arctic Ocean such as iron (Fe). Note that while Fe and Mn share sources, dissolved Fe oxidises more rapidly in absence of organic ligands, hence the extent of its oceanic contribution may be more limited (Landing & Bruland, 1987; Jensen et al., 2020). The oxidation of Mn is largely controlled by microbes (bacteria and fungi) which enhance oxidation kinetics in aquatic environments (Hansel, 2017), in particular near the shelf break (Colombo et al., 2022). Lastly, we can use available Mn observations in the ocean to evaluate the model representation.

In this study, we aim to provide insight into the response of the marine environment to anticipated changes in terrestrial runoff, with a focus on Inuit Nunangat. We trace terrestrial runoff with experiments from a regional Mn model (Rogalla et al., 2022; in review) within a coupled ocean-ice regional model configuration centred on the CAA

(Hu et al., 2018) alongside in situ observations of riverine trace metals collected during the Canadian GEOTRACES cruises in 2015 (Colombo et al., 2019). We separate the runoff sources by type and use simulations from 2002-2020 to study the spatial extent of terrestrial freshwater influence within the CAA to identify regions most strongly impacted by climate change induced runoff composition changes. Then, we consider the implications of runoff composition changes on the quantities of constituents transported downstream to Baffin Bay. The results presented here will help interpret the implications of observed changes to the composition of the Arctic terrestrial freshwater system on the ocean.

2 Methods

In this study, we use a passive tracer model of dissolved manganese (Mn) in the CAA (Rogalla et al., 2022; in review), applied to ocean and ice dynamics from the Arctic and Northern Hemispheric Atlantic configuration (ANHA12; Hu et al., 2018) of the Nucleus for European Modelling of the Ocean (NEMO; Madec, 2008). First we describe the ocean model, then the Mn model.

NEMO is a three-dimensional hydrostatic ocean model that solves the primitive equations on the Arakawa-C grid with a free surface (Madec, 2008). The ocean is coupled to sea ice which is represented using the dynamic and thermodynamic Louvain-la-Neuve (LIM2) model with an elastic-viscous-plastic ice rheology (Fichefet & Maqueda, 1997; Bouillon et al., 2009). However, the ANHA12 simulations do not have a land-fast ice parameterization and so, ice velocities in Parry Channel are higher than observed (Hu et al., 2018; Grivault et al., 2018). Tides are also not included in the current version of the configuration, so polynyas are not always well reproduced (Hughes et al., 2018).

The ANHA12 configuration of NEMO has a 1/12° resolution horizontal grid with a pole in North America, so the resolution effectively corresponds to 2-3 km in Parry Channel. This resolution allows the model to resolve freshwater fluxes associated with coastal currents in the CAA (Bacon et al., 2014; Chelton et al., 1998). The vertical axis is represented by 50 depth levels with highest resolution at the surface (box thickness ranges from 1 m to 454 m for deep basins) and the bottom bathymetry is represented with partial steps. The ANHA12 open boundaries, in Bering Strait and at 20°S in the Atlantic Ocean, are forced with Global Ocean Reanalyses and Simulations data (Masina et al.,

2017). The ocean surface is forced with 10 m hourly atmospheric data from the Canadian Meteorological Centre's global deterministic prediction system (Smith et al., 2014). Terrestrial runoff is based on monthly climatology and around Greenland, runoff is enhanced for melt (Dai et al., 2009; Bamber et al., 2012). The runoff forcing after 2010, repeats the 2010 seasonal cycle. Near large sources such as the Mackenzie River, runoff input is remapped along the shoreline in order to prevent negative salinity artifacts (Hu et al., 2019).

The Mn model is calculated offline on a sub-domain of ANHA12 centred on the CAA (Fig. 1a). The NEMO-TOP engine (Gent et al., 1995; Lévy et al., 2001) calculates the advection and diffusion of Mn based on five-day averaged dynamics fields from a reference experiment of ANHA12 from January 2002 to December 2020. In addition, the Mn model incorporates parameterizations of the sources and sinks that control the distribution of dissolved Mn in the Arctic Ocean: rivers, sediment resuspension, atmospheric dust deposition, dust and sediment flux from sea ice, reversible scavenging, and sinking. The model parameterizations estimate dissolved Mn(II), dMn, and incorporate the indirect effect of lithogenic particles containing Mn through dissolution. Oxidised Mn(IV), oMn, is incorporated to estimate reversible scavenging. With all these components, the model performs well from deep regions in Canada Basin to shallow areas in the CAA. The model does not capture the full variability in near-bottom Mn increases and spatial variation in the magnitude of surface maxima, likely because of the low spatial and temporal resolution of available information for the strongly variable resuspension rates and sea ice sediment content. Here, we will describe the runoff Mn parameterization, since it is the focus of this study. For the full details of the Mn model, see Rogalla et al. (2022; in review).

Terrestrial runoff including river discharge contributes Mn to the shelf seas and into the Arctic Ocean (Colombo et al., 2020; Middag et al., 2011). Mn contributions follow the seasonally fluctuating runoff, Q, and the characteristic concentrations of this runoff vary based on properties of the catchment basins. The CAA is heterogeneous in river composition: glacial rivers have high concentrations of dissolved Mn, rivers draining the continent have intermediate concentrations, and all other rivers have low concentrations (Colombo et al., 2019). The addition of riverine dissolved Mn is estimated as:

$$\frac{\partial [dMn]}{\partial t} = \frac{Q}{\rho_0 \ \Delta z_{surface}} R_{class} \tag{1}$$

where ρ_0 is the density of freshwater and $\Delta z_{surface}$ is the surface grid box thickness. Each runoff source is assigned a class with an associated characteristic trace metal concentration, R_{class}, based on the catchment basin properties (Fig. 1a; Colombo et al., 2019). In the base case, the dMn concentrations are: 164 nM in glacial runoff, 30 nM in continental drainage, and 2 nM in all other runoff. The dMn content for these river categories falls within the lower end of the range of concentrations observed in the Kolyma, Severnaya Dvina, Ob, Lena, and Yenisey, and is compareable to those observed in the Mackenzie River (Holmes et al., 2012; Pokrovsky et al., 2010; Hölemann et al., 2005). In addition to the dissolved Mn content of runoff, Mn can be indirectly added through the dissolution of Mn bounded to particulate matter. We chose not to include the particle-bound contribution, as we were unable to constrain the most representative contribution from suspended matter from the limited observations and since a larger portion of the particulate fraction is typically removed in estuaries (Rogalla et al., 2022; in review; Gordeev et al., 2022). While the treatment of suspended matter presents a limitation on the absolute magnitude of contributions, the relative additions and spatial extents are robust against this choice and our experiment with seasonally varying Mn in runoff gives an indication of the potential impacts of larger riverine Mn contributions.

While there is clear evidence of the cycling of Mn in estuaries, this behaviour varies strongly across regions and by season (Turner et al., 1991; Paucot & Wollast, 1997; Zhou et al., 2003; Gordeev et al., 2022). Given the limited information available to quantify the necessary processes and the resolution of our model, we did not include this aspect in our study. Instead, we focus on estimating the spatial extent and the relative contributions of the rivers on the Mn signature in the ocean which are mostly independent of the magnitude of the contribution.

2.1 Experimental Design

We performed four numerical experiments with the Mn model running from January 2002 to December 2020, altering only the terrestrial runoff Mn forcing (Table 1). Each experiment is spun up by repeating the year 2002 three times, after which the year-to-year change in Mn profiles at evaluation stations is minimal (Fig. S1).

We assess the impacts of changes to the Arctic terrestrial freshwater system on Mn in the ocean and their regions of influence relative to a "base case." In the base case, we

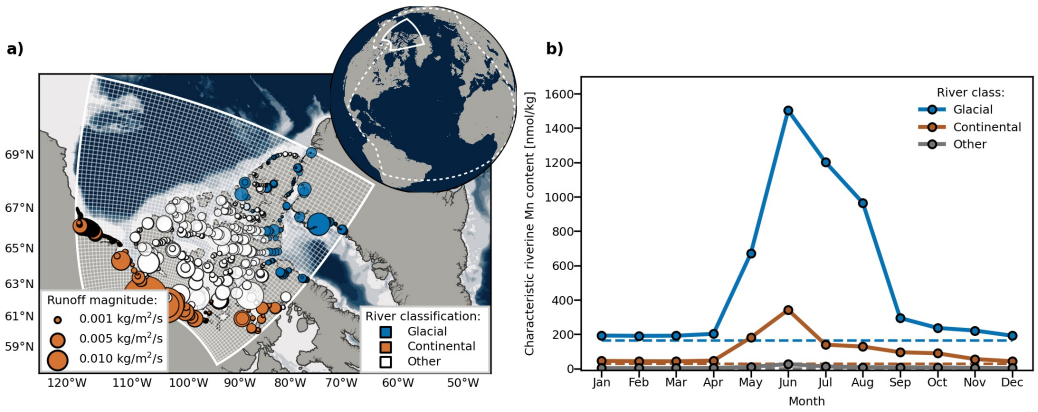

Figure 1. (a) Runoff sources in the model are grouped based on whether they drain glaciers (blue), the continent (brown), and the rest (white). The size of the markers is proportional to the discharge in September (scale indicated on the figure), 2015 from the ANHA12 model forcing (Ferry et al., 2012; Dai et al., 2009). Note that the river mouths are remapped. The dashed line on the inset globe corresponds to the full ANHA12 domain. The boundary of the ANHA12 sub-domain for the Mn model is indicated with a thick white line on both maps and the horizontal resolution of the grid is shown with a thin white line for every ten gridpoints. The background shading represents the model bathymetry. (b) Mean characteristic Mn content, R_{class} (Eqn. 1), of all runoff sources in the domain. Dashed lines represent the base characteristic Mn content for each runoff type. Solid lines indicate the seasonally varying Mn content projections based on Colombo et al. (2019).

used the standard riverine Mn concentrations from observations in the CAA (Colombo et al., 2019). In the "glacial" experiment, we increased Mn concentrations in runoff draining glacial regions by 50% to emulate the increased contribution of micronutrients as a result of enhanced glacial melt (R_{class} in Eqn. 1); we did not alter the river discharge. For the "continental" experiment, we increased Mn concentrations in continental runoff by 50% to emulate the increased contribution of trace metals from permafrost thaw and a stronger groundwater contribution. Although most rivers in Inuit Nunangat drain permafrost covered areas, we chose to increase concentrations only in sources draining the continent, since these regions drain permafrost-covered catchment basins that extend southwards, and thus may see the greatest change in the near decades. In addition to the above experiments, we ran a "seasonal" base case experiment to look at the projected upper maximum seasonal contribution. Using seasonal observations of discharge and Mn concentrations in the Kolyma river, Colombo et al. (2019) projected that Mn concentrations at peak flow could be up 1280% those of low flow. In the "seasonal" experiment, we scale river Mn content so that at peak flow, river concentrations are 1280% the base concentrations and at low flow they are equal to the characteristic concentrations of the other experiments (Fig. 1b). We assume that Mn observations in Colombo et al. (2019) were collected during the low flow season.

Table 1. Terrestrial runoff forcing experiments performed with the Mn model.

Experiment name	Description of runoff forcing	Period
Base	Base Mn content classification	2002-2020[a]
Glacial	Mn content in glacial runoff enhanced by 50%	2002-2020[a]
Continental	Mn content in continental drainage enhanced by 50%	2002-2020[a]
Seasonal	Seasonally varying Mn content in runoff	2002-2020[a]

[a]Prior to the study period, the model is spun up by repeating the year 2002 three times.

2.2 Analysis

We assess the spatial extent of runoff impact on the coastal ocean by calculating the difference in Mn concentration between the "base" experiment and the experiments

with a particular runoff type enhanced ("continental", "glacial" or "seasonal"):

$$P_{exp} = \frac{Mn_{exp} - Mn_{base}}{Mn_{base}} \cdot \frac{1}{f_{exp} - 1} \cdot 100\% \tag{2}$$

where f is the enrichment factor of the Mn runoff forcing in the experiment (for example, 1.5 for a 50% increase in characteristic Mn concentration above the base case), and P is the percent that the specified river type contributes above the "base" experiment Mn concentration. The enrichment factor is incorporated so that when P is 100% at a particular grid cell, all the Mn in this cell is from the runoff that was increased in this experiment.

The fluxes of river-derived Mn were calculated across three main flow pathways from the Arctic Ocean towards the North Atlantic through the CAA: Nares Strait, Baffin Bay, and Parry Channel (boundaries in Fig. 2a). The boundaries lie along lines of constant model grid i or j indices. The Mn flux, ϕ_{bdy}, is the sum of the dissolved Mn concentration at boundary grid cells with indices i, j, k, multiplied by the volume flux calculated from the velocity perpendicular to the boundary, u, and the grid cell area A:

$$\phi_{bdy}(t) = \sum_{i,j,k} [dMn]_{i,j,k}(t) \cdot u_{i,j,k}(t) \cdot A_{i,j,k} \tag{3}$$

where t is the time index of the five-day averaged modelled velocity and Mn fields. Modelled fields were interpolated onto the U grid for the Baffin Bay and Parry Channel boundaries, and onto the V grid for the Nares Strait boundary. The boundary transports from the experiments were compared to the case with base river classification and the difference is represented as a percent (similar to Eqn. 2).

3 Results

Rogalla et al. (2022; in review) found that within the Canadian Arctic Archipelago (CAA), resuspended sediments (40-58%) and sediment released by sea ice (26-37%) are the main external sources of Mn. Terrestrial runoff accounts for 5-34% of external Mn addition across the CAA and is particularly important along coastlines and on regional scales. In this study, we investigate the influence of terrestrial runoff on the ocean in the CAA with experiments from the Mn model (Rogalla et al., 2022; in review) developed with observations from the rivers (Colombo et al., 2019) and the channels (Colombo et al., 2020). In our descriptions, terrestrial freshwater refers to river discharge and surface runoff from land in both glaciated and continental regions (as categorized in Fig. 1a),

and does not include the "other" river category whose influence on Mn is small as illustrated by the "seasonal" experiment. Glacial freshwater is supplied by glacial melt and rivers draining glaciated areas. Continental freshwater originates from rivers and surface runoff from the North American continent.

3.1 The Spatial Extent of Glacial and Continental Runoff

Each type of terrestrial freshwater source in the CAA has a unique spatial fingerprint of influence (Fig. 2). There is a distinct north-south separation between the continental and glacial runoff influenced regions based on the river classification (Fig. 1a, 3). In the following paragraphs, we describe these fingerprints and their overlap based on climatology from 2002-2020.

The "glacial" runoff sources affect inlets of the northwestern CAA, the coast of Baffin Island, and the Arctic waters transported through Nares Strait into Baffin Bay (Fig. 2a), and the strongest contributions are found near coastlines. In Nares Strait, Mn from glacial runoff forms a band of $> 20\%$ contribution along the Greenland coast and in Kane Basin. A plume extends from Kane Basin south through Smith Sound, where it separates from the Greenland coastal band (Fig. 2d) and is entrained by the West Greenland Current. Runoff from Ellesmere Island extends predominantly westward along the continental shelf of the Canada Basin. Along the east coast of Ellesmere Island, the near-shore contributions are lower ($< 8\%$) and are diluted by outflow from the Arctic Ocean. Across Baffin Bay (Fig. 2e), the strongest glacial contributions ($> 15\%$) occur within 20 km of the coasts and down to 50 m depth, while a deeper and less strong glacial signature is visible towards the interior of Baffin Bay around 400 km from Baffin Island and originating from west of Savissivik on Greenland. Near Baffin Island, local glacial rivers contribute to a near shore maximum, while the influence from more distant Nares Strait outflow extends 200 km offshore and to 50-200 m depth (Fig. 2e). Continental river runoff from Parry Channel has a small additional contribution ($< 1\%$) at 20-250 m depth near the Baffin Island coast (Fig. 2e).

Lancaster Sound, the gateway between Parry Channel and Baffin Bay, is influenced by both glacial and continental runoff (Fig. 2b, c). The prevailing direction of flow through Lancaster Sound is eastward (dashed black line in Fig. 2c) and the core of this current transports continental runoff that originates from the southern CAA and recirculating

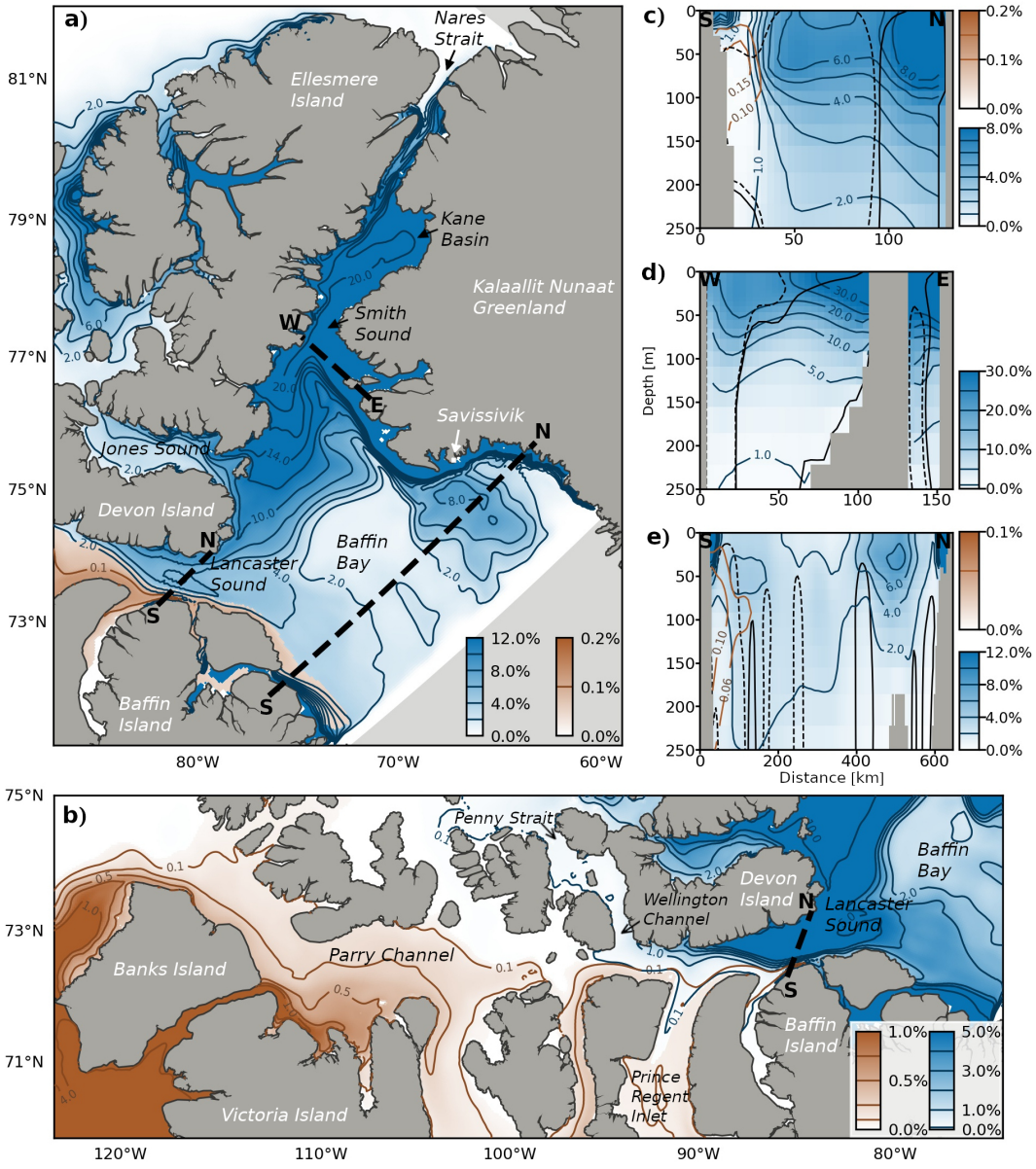

Figure 2. Continental (brown) and glacial (blue) terrestrial freshwater influences geographically distinct regions of the Canadian Arctic Archipelago as highlighted by the September climatological average of the runoff contributions to the upper 34 m of the water column for the northeastern Archipelago (a) and Parry Channel (b). Runoff contributions are calculated as the percent increase of dissolved Mn for the glacial and continental enhanced experiments, relative to the reference run; Eqn. 2. These patterns are characteristic of the full model time period. We show the cross sections of continental and glacial runoff contributions in Lancaster Sound (c), Smith Sound (d), and Baffin Bay (e); boundaries are indicated with dashed black lines in panels a and b. Dashed black contours in the cross sections represent volume fluxes in 2015 directed out of the page, while solid black contours are directed into the page (correspond to 400 m^3 s^{-1} for panels c-d and 2500 m^3 s^{-1} for panel e).

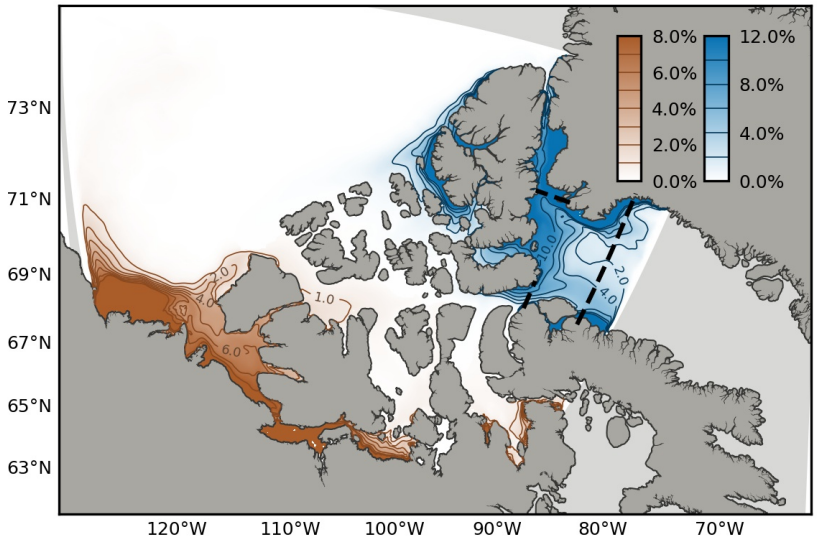

Figure 3. Continental (brown) and glacial (blue) terrestrial freshwater extent in the Polar Mixed Layer (upper 34 m of the water column) in the Canadian Arctic Archipelago, averaged from 2002 to 2020. The percent contributions are calculated as the increase of dissolved Mn in the continental and glacial enhanced experiments, relative to the reference run; Eqn. 2. Regions outside of our sub-domain are colored light gray.

glacial runoff that has spread to central Lancaster Sound. The continental water core extends from the surface down to about 150 m. At these depths, other sources such as sediment resuspension can also contribute Mn (Rogalla et al., 2022; in review). Nares Strait outflow and local sources from Devon Island contribute glacial Mn to the westward return flow in northern Lancaster Sound. This influence can reach as far west as Wellington Channel and extends well below 150 m. On the southern side of Lancaster Sound, local sources from Baffin Island contribute to a shallow glacial band that extends 10 km offshore and to 30 m depth. In October and November, glacial runoff contributions extend from the North side of Lancaster Sound to the central and southern part of the channel (Fig. 4) and are transported eastward by the geostrophic flow from the Arctic Ocean towards Baffin Bay (Fig. 2c).

Continental runoff dominates the southern CAA and central Parry Channel (Fig. 2b, 3). The largest continental river in our domain is the Mackenzie River, nearby the western boundary. The dominant direction of the Mackenzie River plume is eastward towards the CAA, however, strong westward wind events can drive the plume into the Canada

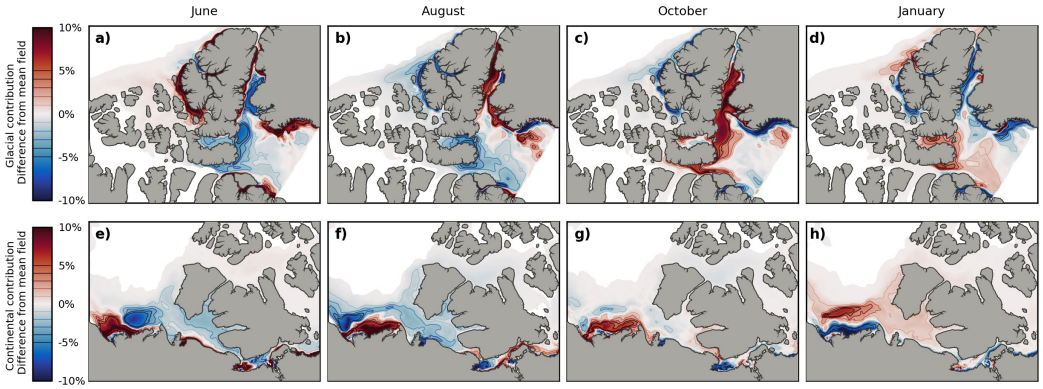

Figure 4. Snapshots of seasonal variations in the extent of glacial (panels a-d) and continental (panels e-h) terrestrial freshwater in the Polar Mixed Layer (upper 34 m of the water column) in the Canadian Arctic Archipelago, based on monthly climatology from 2002 to 2020. The colorbar indicates seasonal increases (red) and decreases (blue) in glacial (panels a-d) and continental (panels e-h) contribution as a percent change from the mean field in Fig. 3.

Basin (Fig. 5). The Mackenzie River plume can extend over 400 km to the east of the river mouth and its effect is visible 200 km offshore. The highest continental contributions are found in the southwestern CAA ($> 10\%$). Overall, the continental runoff contributions are smaller and more diffuse than that of the glacial runoff. Continental runoff travels through Prince Regent Inlet and around Banks Island into central Parry Channel where the overall continental contribution is widespread and around 0.1-0.5% (Fig. 2b). The continental-origin terrestrial freshwater extends north of Parry Channel in the northwest corner of the CAA for part of the year. The distributions of continental runoff follow circulation pathways highlighted by pollutant dispersion experiments in Tao and Myers (2022).

While the overall north-south separation in continental and glacial origin freshwater is present throughout the year (Fig. 3), there are month-to-month variations in the location and magnitude of contributions (Fig. 4, S2-3).

The seasonal variations in continental runoff contributions are most apparent on the Beaufort Shelf and in Parry Channel (Fig. 4, S3). The Mackenzie River drives the continental contribution on the Beaufort Shelf and dominates all other continental river sources. The minimum offshore extent of the continental contribution, 150 km, occurs in July and August. Starting in October and throughout the winter, continental runoff

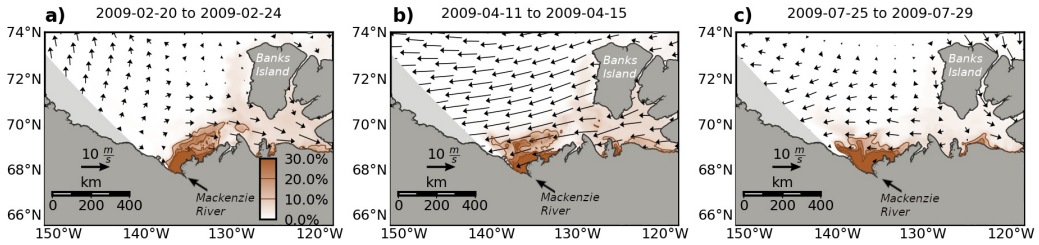

Figure 5. The Mackenzie River dominates continental runoff contributions along the Beaufort Shelf and the plume direction is affected by wind forcing as demonstrated through three five-day example periods in 2009 (panels a-c). Runoff contributions are calculated as the percent increase of dissolved Mn for the continental enhanced experiment, relative to the reference run for each five-day period (Eqn. 2) and averaged over the upper 34 m of the water column. Arrows indicate wind direction and speed at 10 m above the ocean based on the Canadian Meteorological Centre's global deterministic prediction system (Smith et al., 2014), averaged over the five-day date ranges.

is pushed offshore. These months are associated with westward wind events that drive upwelling on the shelf and offshore transport (Stegall & Zhang, 2012). Continental runoff reaches its maximum extent, 375 km offshore, by March. During the winter months (December to March), western Parry Channel also retains a weak but increased continental contribution signature.

Glacial runoff contributions vary seasonally around Ellesmere Island, the Greenland coast, Nares Strait, Lancaster Sound, and in Baffin Bay (Fig. 4, S2). Runoff contributions from Ellesmere Island extend along the northwest coast 100 km offshore from December through May. During these months, runoff contributions in Nares Strait are diminished due to a combination of low discharge rates and strong Arctic Ocean inflow. Starting in June, we see strong coastal increases in glacial contributions along western Nares Strait and in the following months, central Nares Strait receives strong contributions from both Greenland and Ellesmere Island. In September, more of the Nares Strait runoff contributions extend southward into Baffin Bay. Runoff from the coast of Greenland along Baffin Bay is strongest March through June and separates from the cape near Savissivik and is transported into Baffin Bay from June to August (signature present in September-October as well; Fig. 2a, S2f-h). From October through February, the contribution of glacial runoff extends into northern Lancaster Sound and in October and

November extends as far west as Wellington Channel. Within Lancaster Sound, glacial contributions are transported eastward with the dominant flow direction into Baffin Bay where they incorporate into the southward flowing Baffin current. Local Baffin Island glacial runoff is strongest from May to July and remains near the Baffin Island coast.

3.2 Time Series of Runoff Contributions to Mn Transport Through Main Pathways

Time series of fluxes of Mn are calculated across three main cross-sections from the Arctic Ocean to the North Atlantic through the CAA: Nares Strait, Baffin Bay, and Parry Channel (Fig. 6, S7; boundaries in Fig. 2a). We compare the transports calculated from the sensitivity experiments relative to the base run following Eqn. 2. The physical dynamics are the same for all experiments, so any differences are indicative of a change in supply. Interannual variations are associated with changes in routing.

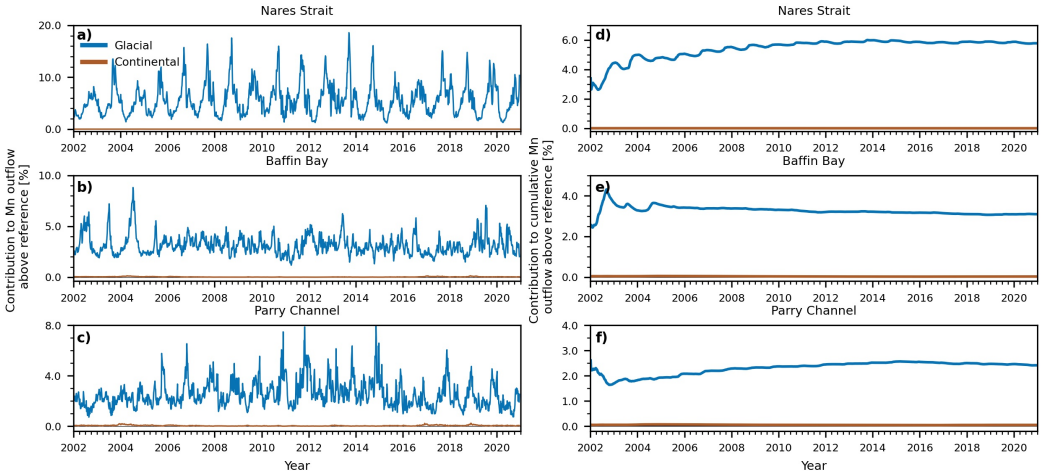

Figure 6. Time series of instantaneous (panels a-c) and cumulative (panels d-f) enhanced Mn outflow (eastward and southward) in glacial melt (blue) and permafrost thaw (brown) experiments at important flow pathways (boundaries shown in Fig. 2a). Fluxes are calculated over the full water column from five-day velocity and tracer fields and compared with the reference run (Eqn. 2). Glacial and continental runoff contributions vary seasonally (scaled time series in Fig. S10a-c). Note the different vertical axis scales.

There are no strong temporal trends in runoff contributions to Mn outflow between 2002-2020 (Fig. 6d-f). Note that the runoff forcing after year 2010 is repeated for the

rest of the time series, so any changes from 2010-2020 would be related to transport differences instead of supply. A gradual increase in glacial contributions is apparent in Nares Strait from 2002-2014 (Fig. 6d). Similarly, although small in magnitude, the glacial contributions to Parry Channel increase from 1.5% in 2003 to 2.4% in 2014 and remain constant from 2014-2020. Throughout the time series, continental runoff contributions are negligible across the Parry Channel, Baffin Bay, and Nares Strait boundaries, relative to glacial contributions (Fig. 6). Continental runoff typically contributes around 0.05% to Mn outflow at Parry Channel and Baffin Bay. The greatest continental contributions occur in Parry Channel (up to 0.2%) in December 2004, 2017, and 2019, with coincident increases in the Baffin Bay outflow.

Runoff contributions to Mn outflow are most important for Nares Strait, with glacial runoff contributing 4-6% and varying strongly seasonally (Fig. 6a, d). Glacial runoff contributions are greatest in September-October reaching up to 18% about three months after peak runoff, and drop to around 2% in March-May (Fig. 1b, 4c, S2). Southward glacial Mn transport through Baffin Bay is greatest in July in 2002-2005, just after peak runoff and prior to the peak in Nares Strait outflow (Fig. 6a-b). The seasonal cycle of runoff contributions to Baffin Bay is less coherent from 2006-2020 (Fig. 6b). The cumulative contribution of glacial runoff to Baffin Bay is around 2.9% (Fig. 6e).

Runoff contributions to Mn flux at Parry Channel are lower than at the other boundaries (Fig. 6c, f). This difference is likely driven by the relative distance of this boundary from strong Mn runoff sources, as oxidation and sinking of Mn removes contributions, and the importance of other sources of Mn. Instantaneously, glacial contributions typically range from 1-3% with some strong seasonal peaks up to 8% (Fig. 6c). Higher glacial contributions to Mn outflow from Parry Channel are seen in October; the months where Nares Strait glacial runoff extends into Lancaster Sound (Fig. 4, S2).

3.3 Impact of Seasonally-Varying Content of Runoff

Trace element concentrations in Arctic rivers vary seasonally with discharge as snow melt flushes top-soils during the spring freshet (Bagard et al., 2011; Hölemann et al., 2005). Observational time series of riverine Mn are lacking in the CAA, however Colombo et al. (2019) estimated an upper bound on potential concentrations using the Kolyma river as a proxy. Our "seasonality" experiment incorporates this information into an alternate

river forcing where Mn concentrations at peak flow are 1280% those during the low flow season and the base river classification (Fig. 1b). With this experiment, we found that the spatial variation in monthly runoff contributions on the ocean are similar for both constant and seasonally varying characteristic Mn concentrations in runoff by comparing regions impacted by predominantly one runoff type (Fig. 4, S2-6). The proportion of contributions to the mean field are also comparable (Fig. 3, S4). These similarities are indicative of the importance of the freshet in controlling the spatial distribution of the impacts of runoff. Runoff contributions during low flow season appear lower in the seasonality experiment (Fig. S2-3, S5-7), however this is an artefact from the normalization based on the 1280% increase at peak flow (f_{exp} in Eqn. 2). The overall oceanic influence of runoff on Mn scales proportional to the increase of riverine concentrations associated with peak discharge, however the magnitude is not exactly 12.8 times the estimates from the base river classification (Fig. 6, S7). Runoff contributions to Mn transport across the boundaries is about half the base experiment when scaled by peak flow, suggesting that a doubling of concentrations at peak flow has a net impact on transport of half that. The seasonal cycle of the transport across the boundaries is more pronounced in the "seasonality" experiment, however the timing of extrema is unchanged (Fig. S7).

4 Discussion

Rivers connect terrestrial and marine ecosystems, conveying water, heat, sediments, carbon, and nutrients to the coastal domain and eventually into the ocean. The magnitude and composition of this terrestrial runoff is changing — the hydrological cycle is accelerating and landscape processes along the river catchment basins are altered (Feng et al., 2021; Frey & McClelland, 2009). In the Arctic, permafrost thaw and glacial ice melt will have increasingly prominent effects on terrestrial runoff composition (Koch et al., 2013; Aiken et al., 2014; Bhatia et al., 2021). These riverine changes have cascading impacts on the ocean, reinforcing the need to identify the oceanic regions most directly impacted by this terrestrial runoff. In this study, we alter runoff input of Mn from glacial draining and extensive continental permafrost covered regions in the CAA in a model to identify oceanic regions most affected by changes and we estimate fluxes downstream to Baffin Bay. These findings will facilitate the interpretation of biogeochemical observations collected in the coastal oceans of the CAA and could help inform the implications of observed basin scale river changes.

4.1 Charting the Oceanic Fingerprint of Terrestrial Runoff

River discharge is transported in the ocean via coastal-trapped, buoyancy driven boundary currents (Münchow & Garvine, 1993). In the Arctic Ocean, these boundary currents flow with landmasses to the right and their width is typically 5-10 km (Rossby radius). The contributions from the many freshwater point sources merge and form the Riverine Coastal Domain (RCD; Carmack et al., 2015; Vannote et al., 1980; Simpson, 1997) that extends along the coastline. Our results effectively visualize the RCD extent by describing the fingerprints of influence of continental and glacial runoff on the ocean in the CAA and on the Beaufort Shelf. First, we compare our simulated terrestrial freshwater extents with hydrographic observations and remotely sensed studies to establish the facilities of the model and this approach. Then, we discuss the seasonal variation and drivers of the extent of influence of terrestrial runoff on the ocean in the CAA.

The extent and variability of continental runoff identified in this study is comparable to hydrographic observations in the Canada Basin from 2010 to 2012 (Shen et al., 2016) and remotely sensed dissolved organic matter distributions from August 2002 to 2009 (Fig. 4 and 5; Fichot et al., 2013). The interior of the Canada Basin is relatively isolated from runoff and has low concentrations of river-derived nutrients (Fig. 3; Shen et al., 2016). Continental runoff extends along the Beaufort Shelf and is dominated by the Mackenzie River plume (Fig. 5; Yamamoto-Kawai et al., 2010). The Mackenzie River plume generally extends eastward towards the CAA, however, it travels westward episodically (Fig. 5; Yamamoto-Kawai et al., 2009). Samples of Dissolved Organic Carbon (DOC), chromomorphic dissolved organic matter (CDOM), and oxygen isotopic composition collected between 2010 to 2012 also indicate westward Mackenzie River extent (Shen et al., 2016, sampling did not extend to the east of the Mackenzie River). An increase in the frequency of these events could contribute to an increase in the freshwater content of Canada Basin (Fichot et al., 2013). However, during our time series, we did not identify an increase in the frequency of the extension of Mackenzie River runoff into the central Canada Basin.

Within the CAA, the riverine domain is dominated by a many local point sources that combine, rather than a few large rivers. In our simulations, continental runoff is prevalent in the southern CAA, while Parry Channel receives weaker riverine contributions (Fig. 2). These patterns are similar to those identified by barium and salinity measure-

ments (Yamamoto-Kawai et al., 2010). As the distance from the source location increases, the terrestrial freshwater influence extends deeper in the water column and is weaker, likely through a combination of processes affecting Mn such as oxidation and removal by sinking, and physical processes such as mixing (Fig. 2c, e). Buoyancy boundary currents have been identified on both sides of channels in the CAA combining hydrographic data and traditional knowledge (Arfeuille, 2001). Our results indicated riverine bands on both shores of Lancaster Sound (Fig. 2a, c). On the north end of Lancaster Sound, a coastal current from Baffin Bay recirculates (Prinsenberg et al., 2009; Wang et al., 2012; Tao & Myers, 2022) with strong contributions from glacial runoff in our study, particularly during late summer months (Fig. 4c). This glacial runoff also appears in observations of trace metals and satellite imagery of this region (Colombo et al., 2020, 2021). In addition to direct glacial discharge, sub-glacial plumes can entrain nutrients from deeper water (Bhatia et al., 2021); the model spatial resolution is not large enough to resolve entrainment at the glacier mouth. However, Bhatia et al. (2021) identified that sub-glacial plumes predominantly entrain macronutrients while micronutrients such as Fe and Mn originate from the glacial discharge which our model includes. The south end of Lancaster Sound, near Baffin Island, is relatively fresh with an increased meteoric water contribution based on its oxygen isotopic composition (Yamamoto-Kawai et al., 2010) and in our study received primarily local glacial freshwater and weaker continental freshwater outflow from the CAA (Fig. 2).

In some strong mixing regions of the CAA, Mn from terrestrial freshwater extends further than advection alone can account for. In western Parry Channel, continental freshwater extends northward counter to the prevailing flow directions (Fig. 2b) and in central Parry Channel, the westward Lancaster Sound return flow supplies glacial freshwater as far west as Wellington Channel where a small portion travels northwards into Penny Strait (Fig. 2b, 4c). These extended ranges of influence appear in regions associated with strong tidal mixing. While the model configuration used in this study does not have tides, the model reproduces the locations of these mixing hot-spots (Hughes et al., 2017) and thus they could contribute to this extension in terrestrial freshwater influence.

Seasonal variations in the extent of terrestrial freshwater in the ocean are affected by the discharge rates. River discharge peaks during the spring freshet, typically starting in mid-May in the Canadian Arctic (Ahmed et al., 2020). The characteristic Mn content of rivers during the freshet sets the magnitude of riverine Mn contributions to the

ocean, as indicated by the increase in oceanic contributions roughly proportional to the concentration at peak discharge in the "seasonality" experiment (see Results section 3.3). The runoff contribution to transport across boundaries was half in the "seasonality" experiment relative to the "glacial" and "continental" experiments when scaled by the runoff Mn content at peak discharge (Fig. S7). This difference suggests that the freshet may contribute about half the annual Mn transport across the boundary, in agreement with estimates that 60% of annual discharge occurs from June to July (Lammers et al., 2001). During the spring freshet, freshwater accumulates along coastlines and can form a strong frontal structure that separates the nearshore and offshore (Fig. 4a, e, S5-6; Moore et al., 1995). From September to April runoff is lower (Fig. 1b), the nearshore of the Beaufort Shelf has a weakened continental freshwater contribution, and runoff accumulated during the summer season is transported offshore (Fig. 4g, h). Where the runoff ends up in the ocean is affected by the timing of the freshet, so the observed shift towards an earlier freshet could impact the oceanic distribution of riverine materials such as Mn (Ahmed et al., 2020).

The redistribution of terrestrial freshwater in the ocean depends on sea ice, winds, and ocean currents, all of which vary seasonally (Macdonald et al., 1995). In our climatology, the freshwater contributions in Nares Strait, Lancaster Sound, and over the Beaufort Shelf remained confined to the nearshore during the summer and spread offshore in the winter months (Fig. 4, S3). The offshore transport is affected by the sea ice extent and the mobility of sea ice (Fig. S9). When sea ice is mobile, wind stress is transferred more directly to the water column (Pickart et al., 2009), while immobile ice tends to widen buoyancy boundary currents because of increased surface-stress from flow beneath the ice (Ingram, 1981; Kasper & Weingartner, 2015). During winter months with full sea ice coverage, continental and glacial runoff are redistributed offshore from the Beaufort Shelf and the northwest coast of Ellesmere Island (Fig. 4c, d; S8-9). In Nares Strait, freshwater distributions are also controlled by the strong ocean currents. An August reduction in sea ice thickness coincides with the spread of freshwater influence into central Nares Strait. The subsequent extension southward in September-December occurs in low-sea ice conditions and follows the Lancaster Sound return flow and geostrophic flow eastwards into Baffin Bay and the southward flowing Baffin current (Fig. 4b, S3, S8). Wind can also direct plumes of freshwater runoff within the ocean. As described in Macdonald et al. (1995), in our "continental" model experiment, the Mackenzie river plume spreads

towards the shelf-break as sea ice retreats (Fig. 4e-f and S9). Without sea ice coverage, winds can directly push and separate the Mackenzie runoff plume from the coast of the Beaufort Shelf (Fig. 5; Mulligan & Perrie, 2019). Based on observations, these winds act to divert the plume on timescales of less than a day and can push the plume offshore by up to 30 km per day (Mulligan & Perrie, 2019).

While our model does not represent estuarine dynamics and has a resolution of a few kilometers, when compared with hydrographic and remotely sensed observations, the model represents the overall riverine flow structure in the ocean on the extensive spatial scale of this study. We discussed the spatial variations of terrestrial freshwater (Fig. 2 and 3) and the drivers of runoff extent in the CAA and the resulting seasonal variations in influence (Fig. 4). Both the spatial variations and seasonality of terrestrial freshwater input have direct consequences on the biology and geochemistry of the Arctic Ocean (Brown, Holding, & Carmack, 2020).

4.2 Glacial and Continental Runoff Supply Micronutrients Directly to the Pikialasorsuaq North Water and Cape Bathurst polynyas

Glacial and continental freshwater feed micronutrients to sensitive areas of the ocean and could thereby affect the magnitude and seasonal cycle of phytoplankton blooms, in particular with enhanced contributions from glacial melt and permafrost thaw (Bhatia et al., 2021; Spencer et al., 2015; Aiken et al., 2014). Terrestrial freshwater influence is present in our domain in areas with polynyas (Hannah et al., 2008) including the well-known Pikialasorsuaq or North Water polynya (PNOW) in northern Baffin Bay and the Cape Bathurst polynya on the Beaufort shelf (Fig. 3, 7). These polynyas are associated with high levels of primary productivity which in turn supports a large biomass of zooplankton (Saunders et al., 2003), fish, and marine mammals including belugas, narwhals, and bowhead whales in the Pikialasorsuaq (Heide-Jørgensen et al., 2013), and an abundance of ringed seals in the Cape Bathurst Polynya (Harwood & Stirling, 1992). The productivity is controlled by the hydrographic and geochemical characteristics of the water which is a function of basin-scale circulation and local inputs from land (Mei et al., 2002; Bring et al., 2016). In our simulations, the PNOW is directly impacted by glacial runoff that originates from Greenland and Ellesmere Island via Nares Strait, while the Cape Bathurst polynya receives contributions from continental runoff downstream of the Mackenzie River (Fig. 3, 7). For the following discussion, note that the ANHA12 sim-

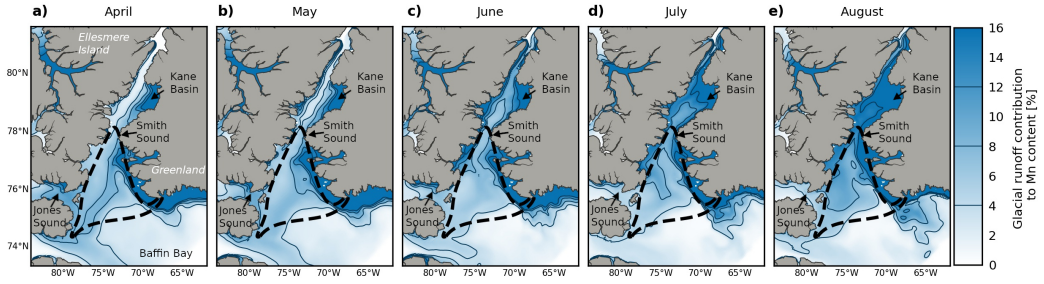

Figure 7. Glacial runoff contributes Mn to highly productive regions in Nares Strait. Panels a-e are climatological monthly glacial runoff contributions to dissolved Mn in the upper 34 m of the water column in the region of the Pikialasorsuaq or North Water polynya, delineated by the dashed black line, from April to August. The contributions are calculated as percent above the reference run (Eqn. 2), averaged monthly between 2002 to 2020. Contour lines are every 4%.

ulation captures the shape of the PNOW polynya well and also simulates the weaker advection of sea ice at Smith Sound and to its south, however the period of ice cover is longer in the model (Hu et al., 2018).

While the start date of the spring bloom in the PNOW is largely controlled by light availability through the retreat of sea ice, nutrients supplied by freshwater runoff sources, such as glacial melt, could help support longer bloom duration. The longest climatological bloom estimated from satellite chlorophyll-a records from 1998-2014 was around 106 days and occurred in Smith Sound, along the Greenland Coast (off Kane Basin) and towards Jones Sound (Marchese et al., 2017). These locations have the earliest bloom start dates, lowest sea ice concentrations, and highest bloom amplitudes (Fig. S8; Marchese et al., 2017). Our model also indicates that these locations receive some of the strongest contributions from glacial runoff during the summer months (Fig. 7). Specifically, in Smith Sound and central Kane Basin, glacial runoff contributes 8-18% to Mn content from June through August, when nutrients typically become limiting and dinoflagellates replace diatoms (Tremblay et al., 2002; Lovejoy et al., 2002). We see notable glacial inputs along the Greenland coast throughout the summer season. The geochemical signature of glacial melt is high in macronutrients such as nitrate and micronutrients such as Fe and Mn, and could thus support productivity (Bhatia et al., 2013, 2021).

A decline in the overall primary production has been observed in the PNOW over the last couple of decades and suggested causes include large-scale changes in the Arc-

tic Ocean such as freshening, heating, or increased stratification, and local scale forcing changes such as surface winds and nutrient supply (Bergeron & Tremblay, 2014; Blais et al., 2017; Marchese et al., 2017). The nutrient inventory of the outflow from the PNOW is also a matter of interest since it is likely to affect the productivity in northern Baffin Bay (Tremblay et al., 2002). In our model simulations, we did not see a significant long term trend in total Mn transport out of Nares Strait across the Smith Sound region from 2002 to 2020 and the composition of this transport also did not significantly change: the total annual glacial Mn transport across the Nares Strait boundary remained relatively constant (Fig. 6d).

4.3 Local Changes to Runoff in Inuit Nunangat may alter the Biogeochemical Composition Downstream in Sub-Arctic Seas

Inuit Nunangat or the Canadian Arctic Archipelago (CAA) accounts for about a third of freshwater export from the Arctic Ocean to the North Atlantic (Haine et al., 2015), second only to Fram Strait in combined liquid and solid freshwater export. As waters transit through the shallow CAA, their composition is altered through strong shelf-ocean interactions and contributions from many freshwater runoff sources (Colombo et al., 2021). As such, local changes to rivers and runoff within the CAA can alter the geochemical and nutrient composition of the CAA outflow, and influence biogeochemical composition downstream in Baffin Bay, the Labrador Sea, and eventually the sub-polar North Atlantic. We estimated glacial and continental runoff contributions to Mn fluxes through the main channels of outflow from Inuit Nunangat: Parry Channel and Nares Strait, and across Baffin Bay (Fig. 6). With these fluxes, we highlight the importance of glacial runoff and estimate how long it takes for glacial and continental runoff changes to feed downstream (Fig. 8).

Runoff released during the spring freshet can take several months to reach key channels such as Nares Strait, Parry Channel, and Baffin Bay, depending on travel distance and routing (Fig. 8, S10). Runoff constituents with geochemical cycling, like Mn, undergo time-dependent scavenging and removal during transit, and so lag times affect the potential of runoff to alter the biogeochemical composition downstream. We estimated the lag times as the difference annually between the peak source discharge and peak runoff contribution in the boundary flux time series (Fig. 6, S10). In Nares Strait, glacial runoff contributions to outflow typically peak around 99 days after peak discharge (i.e. Septem-

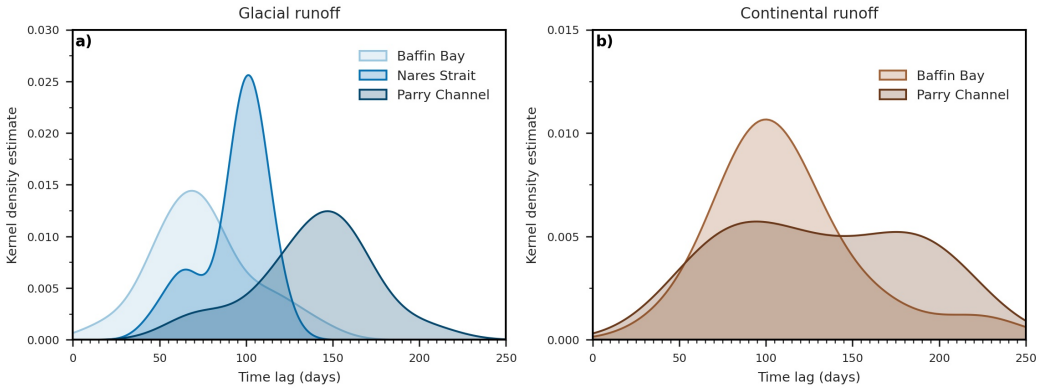

Figure 8. Runoff contributions to downstream Mn fluxes across key channels in the Canadian Arctic peak after the spring freshet. The time lag of the arrival of this maximum depends on the travel distance and route between the runoff sources and the boundaries. We calculated the kernel density estimates of the lag time between peak discharge and peak runoff flux at each of the boundaries for the (a) glacial and (b) continental runoff, based on the flux time series in Fig. 6a-c and S10.

ber), when a plume of glacial runoff extends southward from Nares Strait (Fig. 2a, S5i). The distribution in arrival times in Nares Strait is more tightly constrained than in other passageways (Fig. 8a). In Baffin Bay, glacial runoff arrives from local sources on Baffin Island and Greenland, from upstream areas such as Nares Strait, and through recirculation from Parry Channel (Fig. 2; Gillard et al., 2016); this diversity in source regions is reflected in the broad range of arrival times and a typical arrival time shorter than Nares Strait at 74 days (Fig. 8a). For Baffin Bay, local sources from Baffin Island and Greenland may be more important in determining the peak runoff fluxes than Nares Strait outflow. Parry Channel glacial fluxes peak later than the Nares Strait and Baffin Bay maxima as a result of the late season arrival of Nares Strait glacial runoff via the Lancaster Sound return flow (Fig. 4c).

The continental freshet typically takes around 110 days to reach Baffin Bay and Parry Channel (Fig. 8b, S10e-f), but can take over 200 days, suggesting more potential for removal of geochemical constituents before reaching Baffin Bay compared to glacial runoff. The broad ranges in the continental runoff arrival time in Parry Channel and Baffin Bay likely reflect the larger distance between major runoff sources, such as the Mackenzie river, and the Parry Channel and Baffin Bay boundaries (Fig. 3). However, the broad

range may also be due to the relatively weaker seasonal signal in boundary fluxes (Fig. S10a-c) and the associated smaller number of peaks included in the arrival time estimate. The length of the continental and glacial freshet is comparable in the model forcing (Fig. 1b), so the forcing is unlikely to contribute to the spread in arrival times.

Glacial runoff contributions exceed continental runoff additions to downstream fluxes through all of the CAA channels and can be significant seasonally (Fig. 6). The greater importance of glacial runoff results from reduced removal due to shorter travel distances and arrival times (Fig. 8a), less dilution with many forms of outflow, and larger characteristic Mn concentrations in glacial runoff in our model forcing. Based on our time series, glacial runoff constituent changes contribute about 3-6% to net Mn fluxes across the important boundaries of Parry Channel, Nares Strait, and Baffin Bay annually. However, seasonal fluxes downstream can account for up to 18% of Mn transported across the Nares Strait boundary and up to 8% across Baffin Bay, representing a significant source of Mn (Fig. 6a-b). Continental runoff remains more contained within the southern channels of the CAA, while strong outflow from Nares Strait funnels glacial runoff directly downstream to Baffin Bay (Fig. 3). This difference also suggests that the routing of runoff in this context controls the influence of the runoff on regions downstream.

Future projections indicate that increased phytoplankton nutrient limitation in Baffin Bay will lead to a decline in primary productivity (Kwiatkowski et al., 2019). While glacial runoff is high in macro- and micro-nutrients such as Mn and Fe (Bhatia et al., 2013, 2021), Hopwood et al. (2015) suggest that the physical circulation around Greenland hinders the export of Fe from the coast to the interior basin. However, in this study we saw indirect routing of glacial runoff via Nares Strait and recirculation from Parry Channel which could contribute to micronutrient fluxes into Baffin Bay, highlighting the role of the CAA as a source of micronutrients downstream (Colombo et al., 2021).

4.4 Limitations of Results

The magnitude and spatial distribution of terrestrial runoff in the ocean is affected by confounding environmental changes such as enhanced discharge, the representation of runoff and sea ice in the physical model, model resolution, and the treatment of scavenging, sinking and removal of oxidised Mn, estuarine cycling, and characteristic Mn con-

centrations in runoff in the Mn model. We identify and explain the impact of these factors on the results below.

In this study, we focused on the oceanic impacts of biogeochemical constituent changes in terrestrial runoff, however discharge changes are another aspect of future predictions of the impact of runoff on biogeochemical constituents in the ocean (Peterson et al., 2002; McClelland et al., 2006; Feng et al., 2021) and are certainly an important avenue for further research. Predicted increases in river discharge are associated with stronger stratification, suppression of mixing, and altered ocean dynamics. These factors are likely to increase the magnitude of runoff contributions on the surface ocean and potentially the extent of runoff influence. However, in section 4.1, we identified that runoff influence can extend beyond prevailing current directions in regions associated with strong mixing, suggesting that the suppression of mixing through stronger stratification could reduce the glacial runoff influence to Penny Strait and certain similar areas.

The spatial distribution of runoff in winter is impacted by sea ice (Section 4.1) and in this context, the model representation of sea ice. The model does not include land-fast ice and tides, resulting in more mobile ice than observed. Specifically in the Beaufort Shelf region, the model does not represent the influence of land-fast ice build up which may result in farther offshore freshwater transport in winter than in reality. In observations, offshore transport of freshwater is suppressed by the incorporation of freshwater into landfast ice and the spread of freshwater offshore is limited by the dam-like stamukhi in late winter (Macdonald et al., 1995). In addition, river runoff in the model does not alter ocean heat content, so sea ice near river mouths may be overestimated in the model, suppressing offshore spread of freshwater.

The terrestrial runoff forcing in the physical model does not vary interannually after 2010 and is limited by the number of available stream gauges in the Canadian Arctic (Dai et al., 2009; Bamber et al., 2012). As a result, we may underestimate the runoff contributions to the CAA and downstream fluxes from 2010-2020. However, the dominant circulation patterns and ocean pathways are driven by the Arctic Ocean to North Atlantic pressure gradients and are thus relatively robust against these differences. Coupling of ocean models with runoff forcing derived from hydrological modelling of river catchment basins could improve these estimates. Hydrological model products also may have stronger continental runoff in the CAA than the Dai et al. (2009) dataset. Lastly,

while the 1/12 degree resolution of this configuration allows the representation of freshwater fluxes associated with coastal currents, it is too coarse to represent physical processes associated with the land-ocean interface related to runoff, such as estuarine flow and sub-glacial melt plumes (Bhatia et al., 2021). Nevertheless, when compared with hydrographic and remotely sensed observations (section 4.1), the model represents the overall runoff flow in the ocean on the extensive spatial scale of this study.

Besides the physical factors described above, our estimates of the role of runoff on the ocean are a function of the treatment in the Mn model of: runoff magnitude and characteristic Mn content, estuarine cycling, scavenging and removal through sinking. The concentrations of riverine trace metals are relatively poorly constrained at peak discharge for smaller Arctic rivers. The resulting oceanic influence pattern is unlikely to change, but the magnitude of additions can be greater as highlighted by our "seasonality" experiment. In this study, we chose not to incorporate the estuarine cycling of Mn and instead add only the dissolved fraction in river discharge as larger portions of the dissolved fraction typically make it through the river-sea mixing zone (Gordeev et al., 2022). As discussed in section 4.3, the flux of biogeochemical constituents downstream is also highly dependent on the removal rates, highlighting the need to constrain scavenging and sinking rates, and the factors that they depend on.

While our estimate of the magnitude of influence of terrestrial runoff should be taken as a first order estimate, the key results of the spatial extent and relative role of continental and glacial runoff are robust to the uncertainties described above.

5 Conclusion

Terrestrial runoff is an important source of geochemical constituents to the Arctic Ocean. The concentrations of nutrients in runoff are predicted to increase markedly with permafrost degradation, a transition from a surface water to a groundwater dominated system, and glacial melt (Spencer et al., 2015; Walvoord & Striegl, 2007; Bhatia et al., 2013). However, the extent to which changes to the terrestrial runoff impacts the marine environment is challenging to quantify. In this study, we conducted four experiments with a model of manganese (Mn; Rogalla et al., 2022; in review) in Inuit Nunangat or the Canadian Arctic Archipelago (CAA) from 2002-2020 to identify the extent and magnitude of impact of glacial and continental runoff changes on the ocean of Inuit

Nunangat and the role of runoff changes on downstream fluxes of micronutrients. We found that:

(1) The heterogeneity in geochemical composition of Arctic river types creates distinct patterns of impact on the ocean in the CAA. The spatial extent of continental and glacial runoff contributions vary seasonally with changes in flow patterns, sea ice, and surface winds and the magnitude of the runoff contribution is primarily controlled by the characteristic Mn concentration during the freshet. While recent observations of trace elements in small rivers in the CAA provided a starting point for the terrestrial runoff contribution estimates in this study (Colombo et al., 2019; Brown, Williams, et al., 2020), further measurements of trace element concentrations at peak discharge in small rivers and better constrained estuarine removal rates for dissolved and particulate materials would significantly improve the estimates of the magnitude of runoff contributions on the biogeochemical composition of the ocean.

(2) Terrestrial freshwater feeds micronutrients to two well-known polynyas in our domain: the Pikialasorsuaq or North Water polynya (PNOW) and the Cape Bathurst polynya (Fig. 3, 7). Glacial runoff is rich in macro- and micro-nutrients such as Mn (Bhatia et al., 2013, 2021) and its presence in polynyas could help support high productivity rates. In our experiments, glacial runoff extends into the PNOW during late summer months when nutrients typically become limiting and may help support the long phytoplankton bloom durations and large bloom magnitudes observed in Kane Basin, Smith Sound, and the PNOW region (Marchese et al., 2017).

(3) Glacial runoff dominates continental runoff changes to downstream fluxes through the main channels of the CAA and may alter the biogeochemical composition of regions downstream. Local changes in glacial runoff contribute around 6% annually to Mn fluxes out of Nares Strait, but account for up to 18% seasonally. This seasonal peak is associated with the freshet and takes several days to months to reach the Nares Strait, Parry Channel, and Baffin Bay boundaries (Fig. 8). These transit times could help estimate reductions to downstream transport of biogeochemical runoff constituents associated with scavenging and removal from the water column. Further studies to constrain removal rates and quantitative estimates of the factors controlling removal will help improve downstream Mn and other micronutrient flux estimates.

Open Research

The Mn model configuration, results, and analysis code are archived on FRDR at https://doi.org/10.20383/103.0599 and the Mn model code is available at https://doi.org/10.20383/102.0388. Analysis code is also available on Github at https://github.com/brogalla/Mn-CAA-terrestrial-runoff. Dissolved and particulate Mn observations in the Canadian Arctic Archipelago are available as part of the GEOTRACES Intermediate Data Product Group (2021) via the British Oceanographic Data Centre: https://www.bodc.ac.uk/geotraces/data/idp2021/. The numerical ocean model, NEMO, is available at https://www.nemo-ocean.eu/ (Madec, 2008). For more details on the Arctic and Northern Hemispheric Atlantic 1/12 degree configuration (ANHA12) of NEMO, visit http://knossos.eas.ualberta.ca/anha/anhatable.php. All analysis was performed using Python 3 (Van Rossum & Drake, 2009) within Jupyter Notebooks with the NumPy, Pandas, Matplotlib, Seaborn, and cmocean packages (Kluyver et al., 2016; Oliphant, 2006; The Pandas development team, 2020; Hunter, 2007; Waskom & the Seaborn development team, 2020; Thyng et al., 2016).

Acknowledgments

The experiments in this study were conducted using computer resources provided by Compute Canada (RRG 2648 RAC 2019, RRG 2969 RAC 2020, RRG 1541 RAC 2021, RRG 1792 RAC 2022). The National Sciences and Engineering Council (NSERC) funded this work through the Climate Change and Atmospheric Research Grant: GEOTRACES (RGPCC 433848-12) and an NSERC Discovery Grant (RGPIN-2016-03865) to SEA. The University of British Columbia funded BR through a four year fellowship. The analysis scripts can be found on Github at https://github.com/brogalla/Mn-CAA-terrestrial-runoff, and the model setup and results can be downloaded from FRDR at https://doi.org/10.20383/103.0599

References

Ahmed, R., Prowse, T. D., Dibike, Y., Bonsal, B., & O'Neil, H. (2020). Recent trends in freshwater influx to the Arctic Ocean from four major Arctic-draining rivers. *Water*, *12*(4), 1189.

Aiken, G. R., Spencer, R. G. M., Striegl, R. G., Schuster, P. F., & Raymond, P. A. (2014). Influences of glacier melt and permafrost thaw on the age of dissolved

organic carbon in the Yukon River basin. *Global Biogeochem. Cycles*, *28*(5), 525-537.

Alkire, M. B., Jacobson, A. D., Lehn, G. O., Macdonald, R. W., & Rossi, M. W. (2017). On the geochemical heterogeneity of rivers draining into the straits and channels of the Canadian Arctic Archipelago. *J. Geophys. Res.-Biogeosciences*, *122*, 2527-2547.

Arfeuille, G. (2001). *On the freshwater transport through the southwest Canadian Arctic Archipelago due to buoyancy and wind forcing* (Doctoral dissertation, University of Victoria). doi: 1828/8792

Bacon, S., Marshall, A., Holliday, N. P., Aksenov, Y., & Dye, S. R. (2014). Seasonal variability of the East Greenland Coastal Current. *J. Geophys. Res.-Ocean.*, *119*(6), 3967-3987.

Bagard, M.-L., Chabaux, F., Pokrovsky, O. S., Viers, J., Prokushkin, A. S., Stille, P., ... Dupré, B. (2011). Seasonal variability of element fluxes in two Central Siberian rivers draining high latitude permafrost dominated areas. *Geochem. Cosmochim. Acta*, *75*(12), 3335-3357.

Bamber, J., Van Den Broeke, M., Ettema, J., Lenaerts, J., & Rignot, E. (2012). Recent large increases in freshwater fluxes from Greenland into the North Atlantic. *Geophys. Res. Lett.*, *39*(19).

Bergeron, M., & Tremblay, J.-É. (2014). Shifts in biological productivity inferred from nutrient drawdown in the southern Beaufort Sea (2003-2011) and northern Baffin Bay (1997-2011), Canadian Arctic. *Geophys. Res. Lett.*, *41*(11), 3979-3987.

Bhatia, M. P., Kujawinski, E. B., Das, S. B., Breier, C. F., Henderson, P. B., & Charette, M. A. (2013). Greenland meltwater as a significant and potentially bioavailable source of iron to the ocean. *Nat. Geosci.*, *6*, 274-278.

Bhatia, M. P., Waterman, S., Burgess, D. O., Williams, P. L., Bundy, R. M., Mellett, T., ... Bertrand, E. M. (2021). Glaciers and nutrients in the Canadian Arctic Archipelago marine system. *Global Biogeochem. Cycles*, *35*(8), e2021GB006976.

Blais, M., Ardyna, M., Gosselin, M., Dumont, D., Bélanger, S., Tremblay, J.-É., ... Poulin, M. (2017). Contrasting interannual changes in phytoplankton productivity and community structure in the coastal Canadian Arctic Ocean. *Limnol.*

Oceanogr., *62*(6), 2480-2497.

Bouillon, S., Morales Maqueda, M. A., Legat, V., & Fichefet, T. (2009). An elastic-viscous-plastic sea ice model formulated on Arakawa B and C grids. *Ocean Model.*, *27*(3-4), 174-184.

Bring, A., Fedorova, I., Dibike, Y., Hinzman, L., Mård, J., Mernild, S. H., ... Woo, M.-K. (2016). Arctic terrestrial hydrology: A synthesis of processes, regional effects, and research challenges. *J. Geophys. Res.-Biogeosciences*, *121*(3), 621-649.

Brown, K. A., Holding, J. M., & Carmack, E. C. (2020). Understanding regional and seasonal variability is key to gaining a Pan-Arctic perspective on Arctic Ocean freshening. *Front. Mar. Sci.*, 606.

Brown, K. A., Williams, W. J., Carmack, E. C., Fiske, G., François, R., McLennan, D., & Peucker-Ehrenbrink, B. (2020). Geochemistry of small Canadian Arctic rivers with diverse geological and hydrological settings. *J. Geophys. Res.-Biogeosciences*, *125*(1).

Carmack, E. C., Winsor, P., & Williams, W. (2015). The contiguous panarctic Riverine Coastal Domain: A unifying concept. *Prog. Oceanogr.*, *139*, 13-23.

Chelton, D. B., DeSzoeke, R. A., Schlax, M. G., El Naggar, K., & Siwertz, N. (1998). Geographical variability of the first baroclinic Rossby Radius of deformation. *J. Phys. Oceangr.*, *28*(3), 433-460.

Colombo, M., Brown, K. A., De Vera, J., Bergquist, B. A., & Orians, K. J. (2019). Trace metal geochemistry of remote rivers in the Canadian Arctic Archipelago. *Chem. Geol.*, *525*, 479-491.

Colombo, M., Jackson, S. L., Cullen, J. T., & Orians, K. J. (2020). Dissolved iron and manganese in the Canadian Arctic Ocean: on the biogeochemical processes controlling their distributions. *Geochem. Cosmochim. Acta*, *277*, 150-174.

Colombo, M., Li, J., Rogalla, B., Allen, S. E., & Maldonado, M. T. (2022). Particulate trace element distributions along the Canadian Arctic GEOTRACES section: shelf-water interactions, advective transport and contrasting biological production. *Geochem. Cosmochim. Acta*, *323*, 183-201.

Colombo, M., Rogalla, B., Li, J., Allen, S. E., Orians, K. J., & Maldonado, M. T. (2021). Canadian Arctic Archipelago shelf-ocean interactions: a major iron

source to Pacific derived waters transiting to the Atlantic. *Global Biogeochem. Cycles*, *35*(10), e2021GB007058.

Dai, A., Qian, T., Trenberth, K. E., & Milliman, J. D. (2009). Changes in continental freshwater discharge from 1948 to 2004. *J. Climate*, *22*(10), 2773-2792.

Feng, D., Gleason, C. J., Lin, P., Yang, X., Pan, M., & Ishitsuka, Y. (2021). Recent changes to Arctic river discharge. *Nat. Commun.*, *12*(1), 1-9.

Ferry, N., Parent, L., Garric, G., Bricaud, C., Testut, C.-E., Galloudec, O. L., ... Zawadzki, L. (2012). *GLORYS2V1 global ocean reanalysis fo the altimetric era (1993 - 2009) at meso scale* (Tech. Rep.). Mercator Ocean. Retrieved from `https://www.mercator-ocean.fr/wp-content/uploads/2015/05/Mercator-Ocean-newsletter-2012_44.pdf#page=28`

Fichefet, T., & Maqueda, M. A. M. (1997). Sensitivity of a global sea ice model to the treatment of ice thermodynamics and dynamics. *J. Geophys. Res.-Ocean.*, *102*(C6), 12609-12646.

Fichot, C. G., Kaiser, K., Hooker, S. B., Amon, R. M. W., Babin, M., Bélanger, S., ... Benner, R. (2013). Pan-Arctic distributions of continental runoff in the Arctic Ocean. *Sci. Rep.*, *3*(1), 1-6.

Frey, K. E., & McClelland, J. W. (2009). Impacts of permafrost degradation on Arctic river biogeochemistry. *Hydrol. Process.*, *23*, 169-182.

Gent, P. R., Willebrand, J., McDougall, T. J., & McWilliams, J. C. (1995). Parameterizing eddy-induced tracer transport in ocean circulation models. *J. Phys. Oceangr.*, *25*(4), 463–474.

GEOTRACES Intermediate Data Product Group. (2021). *The GEOTRACES Intermediate Data Product 2021 (IDP2021)* [Dataset]. NERC EDS British Oceanographic Data Centre NOC. doi: 10.5285/cf2d9ba9-d51d-3b7c-e053-8486abc0f5fd

Gillard, L. C., Hu, X., Myers, P. G., & Bamber, J. L. (2016). Meltwater pathways from marine terminating glaciers of the Greenland ice sheet. *Geophys. Res. Lett.*, *43*(20), 10-873.

Gordeev, V. V., Shevchenko, V. P., Novigatsky, A. N., Kochenkova, A. I., Starodymova, D. P., Lokhov, A. S., ... Yakovlev, A. E. (2022). The River–Sea Transition Zone (Marginal Filter) of the Northern Dvina River as an Effective Trap of Riverine Sedimentary Matter on Its Way to the Open Area of the

White Sea. *Oceanology*, *62*(2), 221-230.

Greene, C. H., & Pershing, A. J. (2007). Climate drives sea change. *Science*, *315*, 1084-1085.

Grenier, M., Brown, K. A., Colombo, M., Belhadj, M., Baconnais, I., Pham, V., ... François, R. (2022). Controlling factors and impacts of river-borne neodymium isotope signatures and rare earth element concentrations supplied to the canadian arctic archipelago. *Earth Planet. Sc. Lett.*, *578*, 117341.

Grivault, N., Hu, X., & Myers, P. G. (2018). Impact of the surface stress on the volume and freshwater transport through the Canadian Arctic Archipelago from a high-resolution numerical simulation. *J. Geophys. Res.-Ocean.*, *123*(12), 9038-9060.

Haine, T. W. N., Curry, B., Gerdes, R., Hansen, E., Karcher, M., Lee, C., ... Woodgate, R. (2015). Arctic freshwater export: Status, mechanisms, and prospects. *Glob. Planet. Change*, *125*, 13-35.

Hannah, C. G., Dupont, F., & Dunphy, M. (2008). Polynyas and Tidal Currents in the Canadian Arctic Archipelago. *Arctic*, *62*, 83-95.

Hansel, C. M. (2017). Manganese in marine microbiology. *Adv. Microb. Physiol.*, *70*, 37-83.

Harwood, L. A., & Stirling, I. (1992). Distribution of ringed seals in the southeastern Beaufort Sea during late summer. *Can. J. Zool.*, *70*(5), 891-900.

Heide-Jørgensen, M. P., Burt, L. M., Hansen, R. G., Nielsen, N. H., Rasmussen, M., Fossette, S., & Stern, H. (2013). The significance of the North Water polynya to Arctic top predators. *Ambio*, *42*(5), 596-610.

Hölemann, J. A., Schirmacher, M., & Prange, A. (2005). Seasonal variability of trace metals in the Lena River and the southeastern Laptev Sea: Impact of the spring freshet. *Glob. Planet. Change*, *48*(1-3), 112-125.

Holmes, R. M., Coe, M. T., Fiske, G. J., Gurtovaya, T., McClelland, J. W., Shiklomanov, A. I., ... Zhulidov, A. V. (2012). Climate Change Impacts on the Hydrology and Biogeochemistry of Arctic Rivers. In C. R. Goldman, M. Kumagai, & R. D. Robarts (Eds.), *Climatic Change and Global Warming of Inland Waters* (p. 1-26). John Wiley and Sons, Ltd.

Hopwood, M. J., Bacon, S., Arendt, K., Connelly, D. P., & Statham, P. J. (2015). Glacial meltwater from Greenland is not likely to be an important source of Fe

to the North Atlantic. *Biogeochemistry*, *124*(1-3), 1-11.

Hu, X., Myers, P. G., & Lu, Y. (2019). Pacific Water Pathway in the Arctic Ocean and Beaufort Gyre in Two Simulations With Different Horizontal Resolutions. *J. Geophys. Res.-Ocean.*, *124*(8), 6414-6432.

Hu, X., Sun, J., Chan, T. O., & Myers, P. G. (2018). Thermodynamic and dynamic ice thickness contributions in the Canadian Arctic Archipelago in NEMO-LIM2 numerical simulations. *Cryosphere*, *12*, 1233-1247.

Hughes, K. G., Klymak, J. M., Hu, X., & Myers, P. G. (2017). Water mass modification and mixing rates in a 1/12 simulation of the Canadian Arctic Archipelago. *J. Geophys. Res.-Ocean.*, *122*, 803-820.

Hughes, K. G., Klymak, J. M., Williams, W. J., & Melling, H. (2018). Tidally modulated internal hydraulic flow and energetics in the central Canadian Arctic Archipelago. *J. Geophys. Res.-Ocean.*, *123*(8), 5210-5229.

Hunter, J. D. (2007). Matplotlib: A 2d graphics environment [Software]. *Comput. Sci. Eng.*, *9*(3), 90–95.

Ingram, R. G. (1981). Characteristics of the Great Whale River plume. *J. Geophys. Res.-Ocean.*, *86*(C3), 2017-2023.

Jensen, L. T., Morton, P., Twining, B. S., Heller, M. I., Hatta, M., Measures, C. I., ... others (2020). A comparison of marine Fe and Mn cycling: US GEOTRACES GN01 Western Arctic case study. *Geochem. Cosmochim. Acta*, *288*, 138-160.

Jickells, T. D. (1999). The inputs of dust derived elements to the Sargasso Sea; a synthesis. *Mar. Chem.*, *68*(1-2), 5-14.

Kadko, D., Aguilar-Islas, A., Bolt, C., Buck, C. S., Fitzsimmons, J. N., Jensen, L. T., ... others (2019). The residence times of trace elements determined in the surface Arctic Ocean during the 2015 US Arctic GEOTRACES expedition. *Mar. Chem.*, *208*, 56-69.

Kasper, J. L., & Weingartner, T. J. (2015). The spreading of a buoyant plume beneath a landfast ice cover. *J. Phys. Oceangr.*, *45*(2), 478-494.

Kluyver, T., Ragan-Kelley, B., Pérez, F., Granger, B., Bussonnier, M., Frederic, J., ... others (2016). *Jupyter Notebooks – a publishing format for reproducible computational workflows* (F. Loizides & B. Schmidt, Eds.) [Software]. IOS Press.

Koch, J. C., Runkel, R. L., Striegl, R., & McKnight, D. M. (2013). Hydrologic controls on the transport and cycling of carbon and nitrogen in a boreal catchment underlain by continuous permafrost. *J. Geophys. Res.-Biogeosciences*, *118*(2), 698-712.

Kwiatkowski, L., Naar, J., Bopp, L., Aumont, O., Defrance, D., & Couespel, D. (2019). Decline in Atlantic primary production accelerated by Greenland Ice Sheet melt. *Geophys. Res. Lett.*, *46*(20), 11347-11357.

Lammers, R. B., Shiklomanov, A. I., Vörösmarty, C. J., Fekete, B. M., & Peterson, B. J. (2001). Assessment of contemporary Arctic river runoff based on observational discharge records. *J. Geophys. Res.-Atm.*, *106*(D4), 3321-3334.

Landing, W. M., & Bruland, K. W. (1980). Manganese in the North Pacific. *Earth Planet. Sc. Lett.*, *49*, 45-56.

Landing, W. M., & Bruland, K. W. (1987). The contrasting biogeochemistry of iron and manganese in the Pacific Ocean. *Geochem. Cosmochim. Acta*, *51*(1), 29-43.

Lévy, M., Estublier, A., & Madec, G. (2001). Choice of an advection scheme for biogeochemical models. *Geophys. Res. Lett.*, *28*(19), 3725–3728.

Lique, C., Holland, M. M., Dibike, Y. B., Lawrence, D. M., & Screen, J. A. (2016). Modeling the Arctic freshwater system and its integration in the global system: Lessons learned and future challenges. *J. Geophys. Res.-Biogeosciences*, *121*, 540-566.

Lovejoy, C., Legendre, L., Martineau, M. J., Bâcle, J., & Von Quillfeldt, C. H. (2002). Distribution of phytoplankton and other protists in the North Water. *Deep Sea Res. Pt. II*, *49*(22-23), 5027-5047.

Macdonald, R. W., Paton, D. W., Carmack, E. C., & Omstedt, A. (1995). The freshwater budget and under-ice spreading of Mackenzie River water in the Canadian Beaufort Sea based on salinity and 18O/16O measurements in water and ice. *J. Geophys. Res.-Ocean.*, *100*(C1), 895-919.

Madec, G. (2008). NEMO ocean engine. *Note du Pôle de modélisation, Institut Pierre-Simon Laplace*, *27*(1288-1619). Retrieved from `https://www.nemo-ocean.eu/wp-content/uploads/NEMO_book.pdf`

Marchese, C., Albouy, C., Tremblay, J.-É., Dumont, D., D'Ortenzio, F., Vissault, S., & Bélanger, S. (2017). Changes in phytoplankton bloom phenology over the

North Water (NOW) polynya: a response to changing environmental conditions. *Polar Biol.*, *40*(9), 1721-1737.

Masina, S., Storto, A., Ferry, N., Valdivieso, M., Haines, K., Balmaseda, M., ... Parent, L. (2017). An ensemble of eddy-permitting global ocean reanalyses from the MyOcean project. *Clim. Dynam.*, *49*(3), 813-841.

McClelland, J. W., Déry, S. J., Peterson, B. J., Holmes, R. M., & Wood, E. F. (2006). A pan-arctic evaluation of changes in river discharge during the latter half of the 20th century. *Geophys. Res. Lett.*, *33*, L06715.

McClelland, J. W., Holmes, R. M., Dunton, K. H., & Macdonald, R. W. (2012). The Arctic Ocean Estuary. *Estuar. Coasts*, *35*, 353-368.

McClelland, J. W., Tank, S. E., Spencer, R. G. M., & Shiklomanov, A. I. (2015). Coordination and sustainability of river observing activities in the Arctic. *Arctic*, *68*, 59-68.

Mei, Z.-P., Legendre, L., Gratton, Y., Tremblay, J.-É., LeBlanc, B., Mundy, C. J., ... von Quillfeldt, C. H. (2002). Physical control of spring-summer phytoplankton dynamics in the North Water, April-July 1998. *Deep Sea Res. Pt. II*, *49*, 4959-4982.

Middag, R., de Baar, H. J. W., Laan, P., & Klunder, M. B. (2011). Fluvial and hydrothermal input of manganese into the Arctic Ocean. *Geochem. Cosmochim. Acta*, *75*(9), 2393-2408.

Moore, S. E., George, J. C., Coyle, K. O., & Weingartner, T. J. (1995). Bowhead whales along the Chukotka coast in autumn. *Arctic*, 155-160.

Mulligan, R. P., & Perrie, W. (2019). Circulation and structure of the Mackenzie River plume in the coastal Arctic Ocean. *Cont. Shelf Res.*, *177*, 59-68.

Münchow, A., & Garvine, R. W. (1993). Dynamical properties of a buoyancy-driven coastal current. *J. Geophys. Res.*, *98*(C11), 20063-20077.

Nijssen, B., O'Donnell, G. M., Hamlet, A. F., & Lettenmaier, D. P. (2001). Hydrologic sensitivity of global rivers to climate change. *Clim. Change*, *50*, 143-175.

Oliphant, T. E. (2006). *A guide to NumPy* (Vol. 1) [Software]. Trelgol Publishing USA.

Paucot, H., & Wollast, R. (1997). Transport and transformation of trace metals in the Scheldt estuary. *Mar. Chem.*, *58*(1-2), 229-244.

Peterson, B. J., Holmes, R. M., McClelland, J. W., Vörösmarty, C. J., Lammers,

R. B., Shiklomanov, A. I., ... Rahmstorf, S. (2002). Increasing river discharge to the Arctic Ocean. *Science*, *298*, 2171-3.

Pickart, R. S., Moore, G. W. K., Torres, D. J., Fratantoni, P. S., Goldsmith, R. A., & Yang, J. (2009). Upwelling on the continental slope of the Alaskan Beaufort Sea: Storms, ice, and oceanographic response. *J. Geophys. Res.-Ocean.*, *114*(C1).

Pokrovsky, O. S., Viers, J., Shirokova, L. S., Shevchenko, V. P., Filipov, A. S., & Dupré, B. (2010). Dissolved, suspended, and colloidal fluxes of organic carbon, major and trace elements in the Severnaya Dvina River and its tributary. *Chem. Geol.*, *273*(1-2), 136-149.

Prinsenberg, S., Hamilton, J., Peterson, I., & Pettipas, R. (2009). Observing and interpreting the seasonal variability of the oceanographic fluxes passing through Lancaster Sound of the Canadian Arctic Archipelago. In J. C. J. Nihoul & A. G. Kostianoy (Eds.), *Influence of Climate Change on the Changing Arctic and Sub-Arctic Conditions* (p. 125-143). Springer Netherlands.

Prowse, T. D., Bring, A., Mård, J., Carmack, E., Holland, M., Instanes, A., ... Wrona, F. J. (2015). Arctic freshwater synthesis: Summary of key emerging issues. *J. Geophys. Res.-Biogeosciences*, *120*, 1887-1893.

Prowse, T. D., & Flegg, P. O. (2000). Arctic River Flow: A Review of Contributing Areas. In E. L. Lewis, E. P. Jones, P. Lemke, T. D. Prowse, & P. Wadhams (Eds.), *The Freshwater Budget of the Arctic Ocean* (Vol. 70, p. 269-280). Springer Netherlands.

Rogalla, B., Allen, S. E., Colombo, M., Myers, P. G., & Orians, K. J. (2022; in review). Sediments in sea ice drive the Canada Basin surface Mn maximum: insights from an Arctic Mn ocean model. *Global Biogeochem. Cycles*. doi: 10.1002/essoar.10507013.3

Saunders, P. A., Deibel, D., Stevens, C. J., Rivkin, R. B., Lee, S. H., & Klein, B. (2003). Copepod herbivory rate in a large arctic polynya and its relationship to seasonal and spatial variation in copepod and phytoplankton biomass. *Mar. Ecol. Prog. Ser.*, *261*, 183-199.

Serreze, M. C., Barrett, A. P., Slater, A. G., Woodgate, R. A., Aagaard, K., Lammers, R. B., ... Lee, C. M. (2006). The large-scale freshwater cycle of the Arctic. *J. Geophys. Res.*, *111*, C11010.

Shen, Y., Benner, R., Robbins, L. L., & Wynn, J. G. (2016). Sources, Distributions, and Dynamics of Dissolved Organic Matter in the Canada and Makarov Basins. *Front. Mar. Sci.*, *3*, 198.

Shiller, A. M. (1997). Manganese in surface waters of the Atlantic Ocean. *Geophys. Res. Lett.*, *24*(12), 1495-1498.

Simpson, J. H. (1997). Physical processes in the ROFI regime. *J. Mar. Sys.*, *12*(1-4), 3-15.

Smith, G. C., Roy, F., Mann, P., Dupont, F., Brasnett, B., Lemieux, J.-F., ... Bélair, S. (2014). A new atmospheric dataset for forcing ice-ocean models: Evaluation of reforecasts using the Canadian global deterministic prediction system. *Q. J. R. Meteorol. Soc.*, *140*(680), 881-894.

Spencer, R. G. M., Mann, P. J., Dittmar, T., Eglinton, T. I., McIntyre, C., Holmes, R. M., ... Stubbins, A. (2015). Detecting the signature of permafrost thaw in Arctic rivers. *Geophys. Res. Lett.*, *42*, 2830-2835.

Stadnyk, T. A., MacDonald, M. K., Tefs, A., Déry, S. J., Koenig, K., Gustafsson, D., ... Olden, J. D. (2020). Hydrological modeling of freshwater discharge into Hudson Bay using HYPE. *Elementa: Science of the Anthropocene*, *8*.

Stegall, S. T., & Zhang, J. (2012). Wind field climatology, changes, and extremes in the Chukchi-Beaufort Seas and Alaska North Slope during 1979-2009. *J. Climate*, *25*(23), 8075-8089.

Sunda, W. G. (2012). Feedback interactions between trace metal nutrients and phytoplankton in the ocean. *Front. Microbiol.*, *3*, 204.

Tank, S. E., Manizza, M., Holmes, R. M., McClelland, J. W., & Peterson, B. J. (2012). The processing and impact of dissolved riverine nitrogen in the Arctic Ocean. *Estuar. Coasts*, *35*, 401-415.

Tao, R., & Myers, P. G. (2022). Modelling the Oceanic Advection of Pollutants Spilt Along with the Northwest Passage. *Atmos.-Ocean*, 1-14.

The Pandas development team. (2020). Pandas-dev/pandas: Pandas [Software]. *Zenodo*, *21*, 1-9.

Thyng, K. M., Greene, C. A., Hetland, R. D., Zimmerle, H. M., & DiMarco, S. F. (2016). True colors of oceanography: Guidelines for effective and accurate colormap selection [Software]. *Oceanogr.*, *29*(3), 9-13.

Tremblay, J.-É., Gratton, Y., Carmack, E. C., Payne, C. D., & Price, N. M. (2002).

Impact of the large-scale Arctic circulation and the North Water Polynya on nutrient inventories in Baffin Bay. *J. Geophys. Res.*, *107*(C8), 3112.

Turner, A., Millward, G. E., & Morris, A. W. (1991). Particulate metals in five major North Sea estuaries. *Estuar. Coast Shelf S.*, *32*(4), 325-346.

Van Hulten, M., Middag, R., Dutay, J.-C., De Baar, H., Roy-Barman, M., Gehlen, M., ... Sterl, A. (2017). Manganese in the west Atlantic Ocean in the context of the first global ocean circulation model of manganese. *Biogeosciences*, *14*, 1123-1152.

Van Rossum, G., & Drake, F. L. (2009). *Python 3 Reference Manual* [Software]. Scotts Valley, CA: CreateSpace.

Vannote, R. L., Minshall, G. W., Cummins, K. W., Sedell, J. R., & Cushing, C. E. (1980). The river continuum concept. *Can. J. Fish. Aquat. Sci.*, *37*(1), 130-137.

Walvoord, M. A., & Striegl, R. G. (2007). Increased groundwater to stream discharge from permafrost thawing in the Yukon river basin: Potential impacts on lateral export of carbon and nitrogen. *Geophys. Res. Lett.*, *34*, L12402.

Wang, Q., Myers, P. G., Hu, X., & Bush, A. B. G. (2012). Flow Constraints on Pathways through the Canadian Arctic Archipelago. *J. Atmos.-Ocean*, *50*(3), 373-385.

Waskom, M., & the Seaborn development team. (2020). *Seaborn* [Software]. Zenodo. doi: 10.5281/zenodo.592845

White, D., Hinzman, L., Alessa, L., Cassano, J., Chambers, M., Falkner, K., ... Zhang, T. (2007). The Arctic freshwater system: Changes and impacts. *J. Geophys. Res.-Biogeosciences*, *112*.

Wrona, F. J., Johansson, M., Culp, J. M., Jenkins, A., Mård, J., Myers-Smith, I. H., ... Wookey, P. A. (2016). Transitions in Arctic ecosystems: Ecological implications of a changing hydrological regime. *J. Geophys. Res.-Biogeosciences*, *121*, 650-674.

Yamamoto-Kawai, M., Carmack, E. C., Mclaughlin, F. A., & Falkner, K. K. (2010). Oxygen isotope ratio, barium and salinity in waters around the North American coast from the Pacific to the Atlantic: Implications for freshwater sources to the Arctic throughflow. *J. Mar. Res.*, *68*, 97-117.

Yamamoto-Kawai, M., McLaughlin, F. A., Carmack, E. C., Nishino, S., Shimada,

1131 K., & Kurita, N. (2009). Surface freshening of the Canada Basin, 2003–2007:
1132 River runoff versus sea ice meltwater. *J. Geophys. Res.*, *114*(C1), C00A05.
1133 Zhou, J. L., Liu, Y. P., & Abrahams, P. W. (2003). Trace metal behaviour in the
1134 Conwy estuary, North Wales. *Chemosphere*, *51*(5), 429-440.

Supporting Information for "Oceanic fingerprints of continental and glacial terrestrial runoff in Inuit Nunangat, the Canadian Arctic Archipelago"

B. Rogalla[1], S. E. Allen[1], M. Colombo[1], P. G. Myers[2], K. J. Orians[1]

[1]Department of Earth, Ocean, and Atmospheric Sciences, University of British Columbia, Vancouver, British Columbia V6T1Z4, Canada

[2]Department of Earth and Atmospheric Sciences, University of Alberta, 1-26 ESB, Edmonton, Alberta T6G2E3, Canada

Contents of this file

1. Figures S1 to S10

Corresponding author: B. Rogalla, Department of Earth, Ocean, and Atmospheric Sciences, University of British Columbia, Earth Sciences Building, Vancouver BC V6T1Z4, Canada. (brogalla@eoas.ubc.ca)

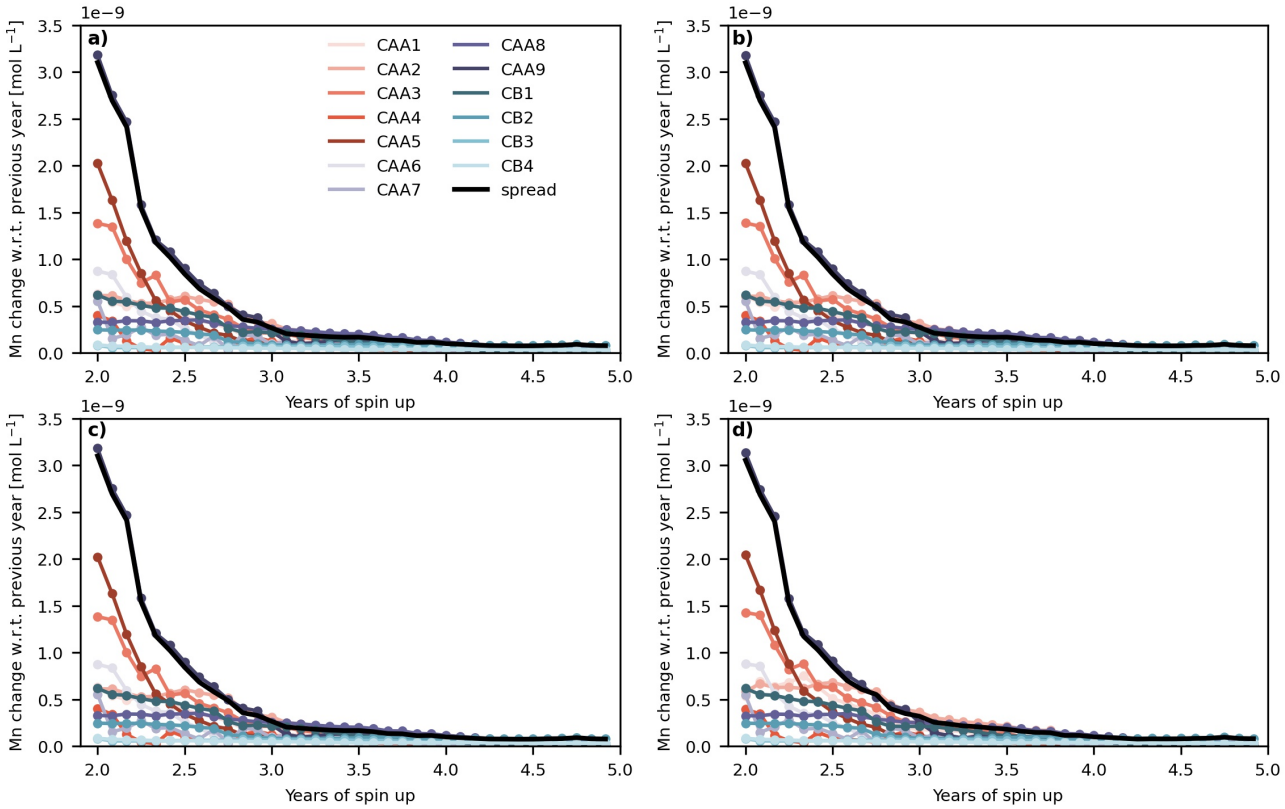

Figure S1. Year-to-year change in Mn concentrations during the three years of model spin up for each of the model experiments in this study, "base" (a), "glacial" (b), "continental" (c), and "seasonal" (d). The Mn model is spun up by repeating the year 2002 until the average Mn difference in the water column at evaluation stations from the 2015 Canadian GEOTRACES cruises (names in legend) is minimal; about three years. The solid black line indicates the difference between the maximum and minimum change at each month.

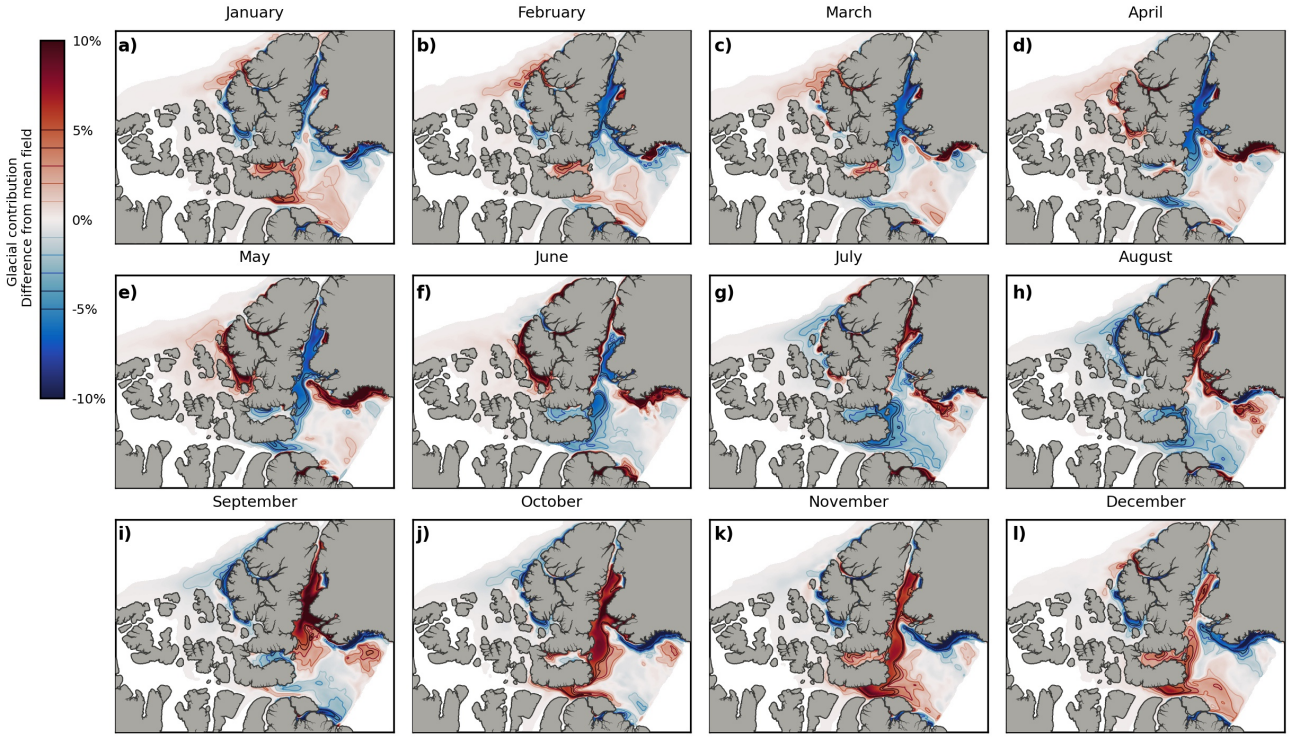

Figure S2. Monthly variations in the extent of glacial terrestrial freshwater in the Polar Mixed Layer (upper 34 m of the water column) in the northeastern Canadian Arctic Archipelago, based on climatology from 2002 to 2020. The seasonal increases (red) and decreases (blue) in contribution are calculated as a percent change from the mean field in Fig. 3.

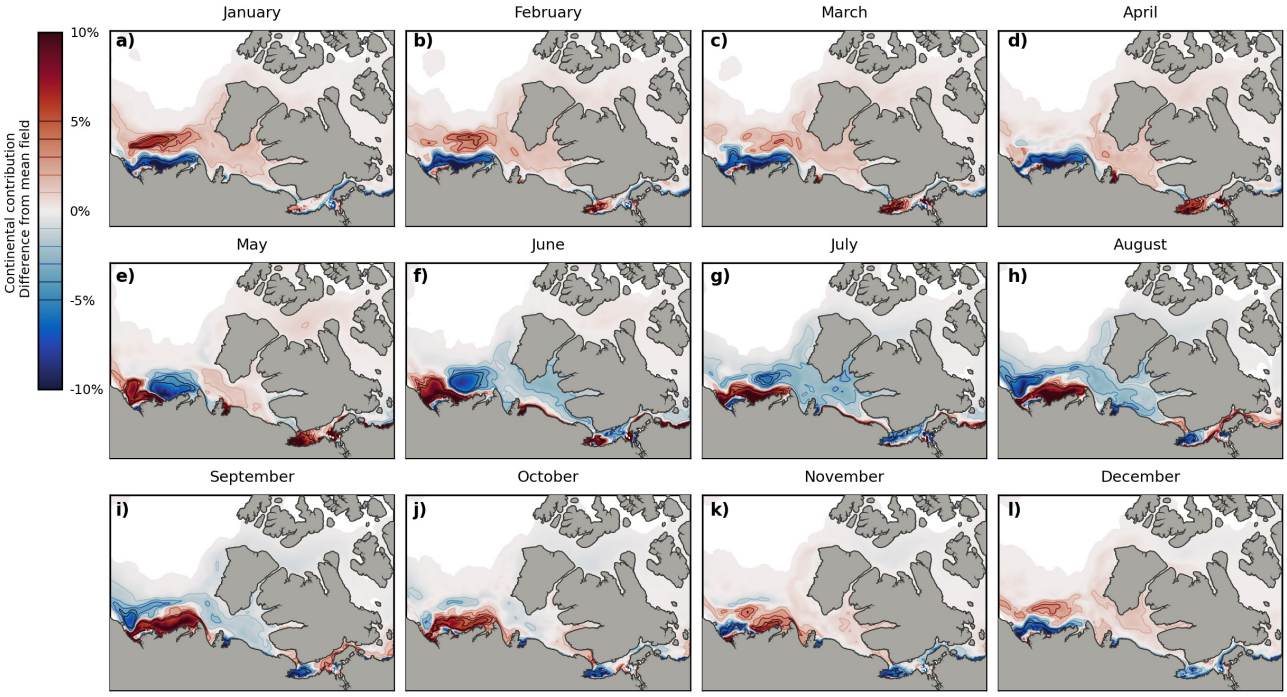

Figure S3. Monthly variations in the extent of continental terrestrial freshwater in the Polar Mixed Layer (upper 34 m of the water column) over the Beaufort Shelf and the southwestern Canadian Arctic Archipelago, based on climatology from 2002 to 2020. The seasonal increases (red) and decreases (blue) in contribution are calculated as a percent change from the mean field in Fig. 3.

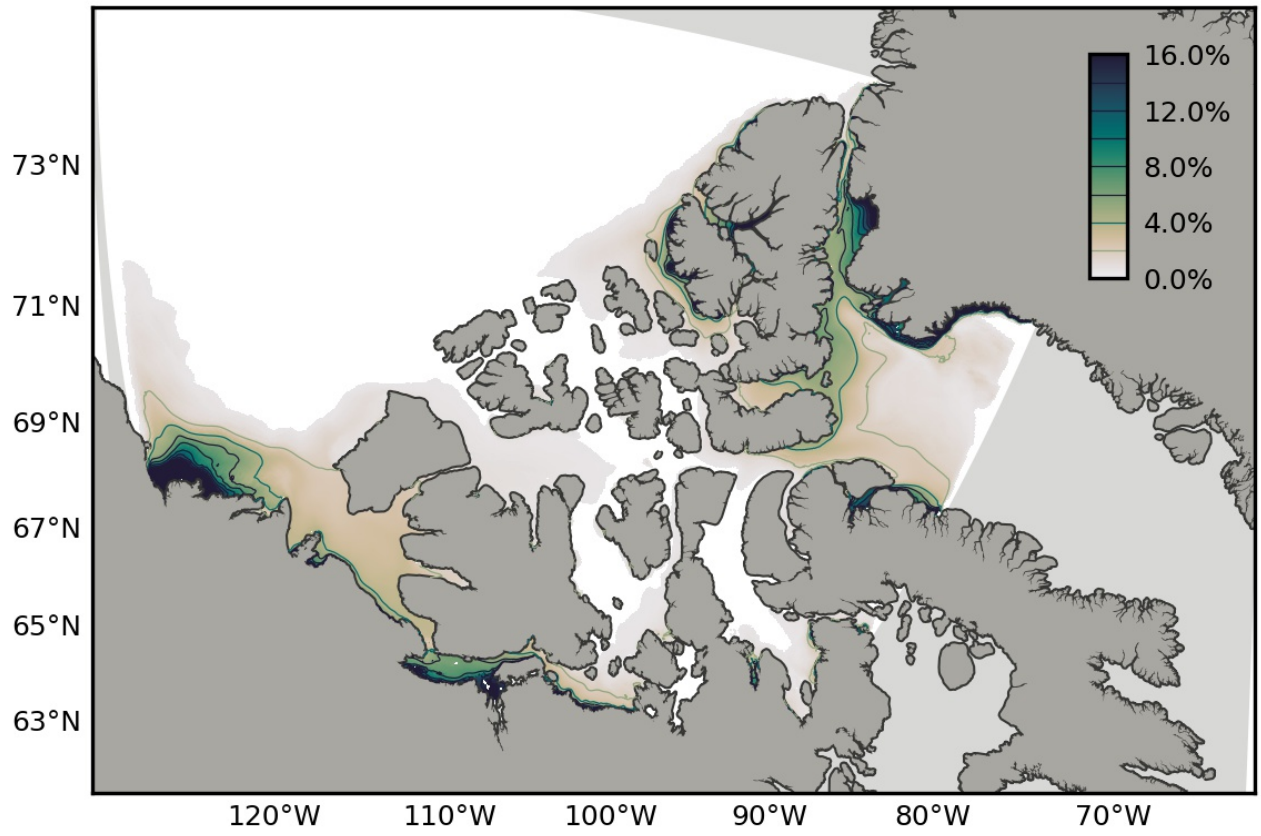

Figure S4. Contribution of terrestrial freshwater to the Polar Mixed Layer (upper 34 m of the water column) in the Canadian Arctic Archipelago in the "seasonality" experiment, averaged from 2002 to 2020. The percent contributions are calculated as the increase of dissolved Mn in the seasonality experiment, relative to the reference run, scaled by the increase in maximum characteristic riverine Mn concentrations (Eqn. 2). Regions outside of our sub-domain are colored light gray.

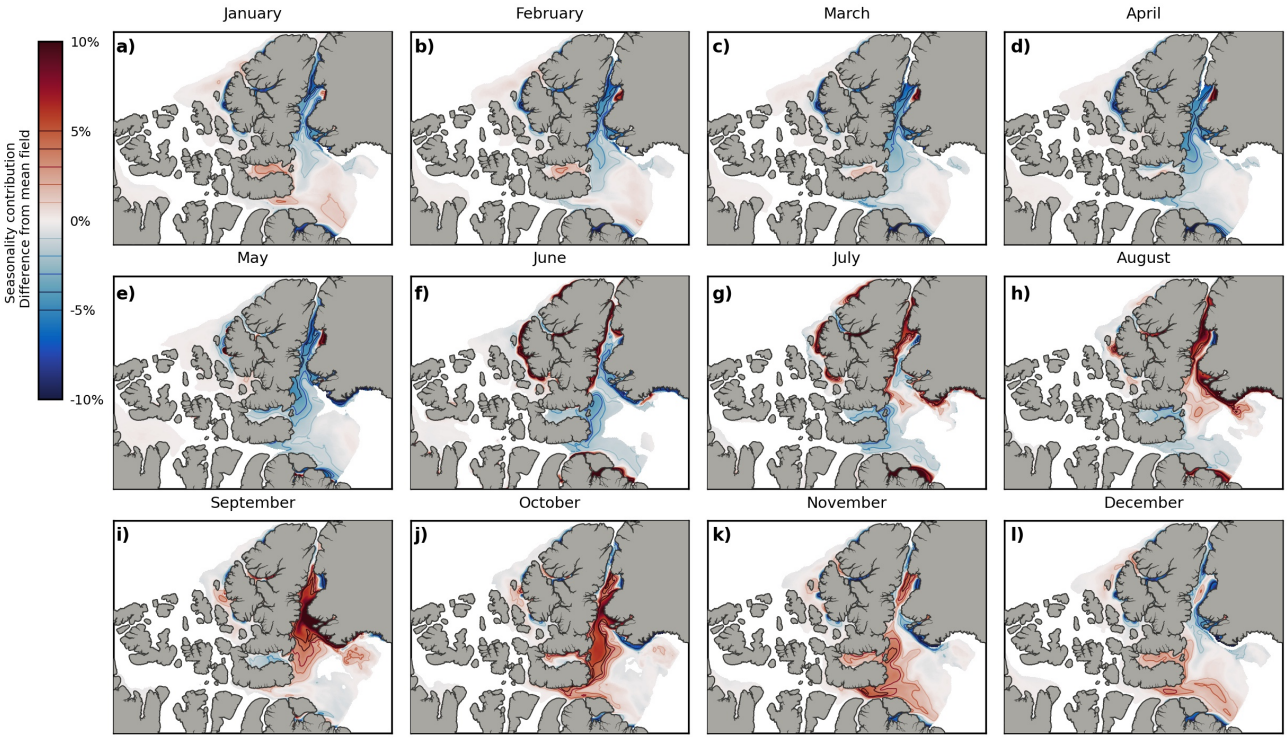

Figure S5. Monthly variations in the extent of terrestrial freshwater in the Polar Mixed Layer (upper 34 m of the water column) in the northeastern Canadian Arctic Archipelago in the "seasonality" experiment, based on climatology from 2002 to 2020. The seasonal increases (red) and decreases (blue) in contribution are calculated as a percent change from the mean field in Fig. S4

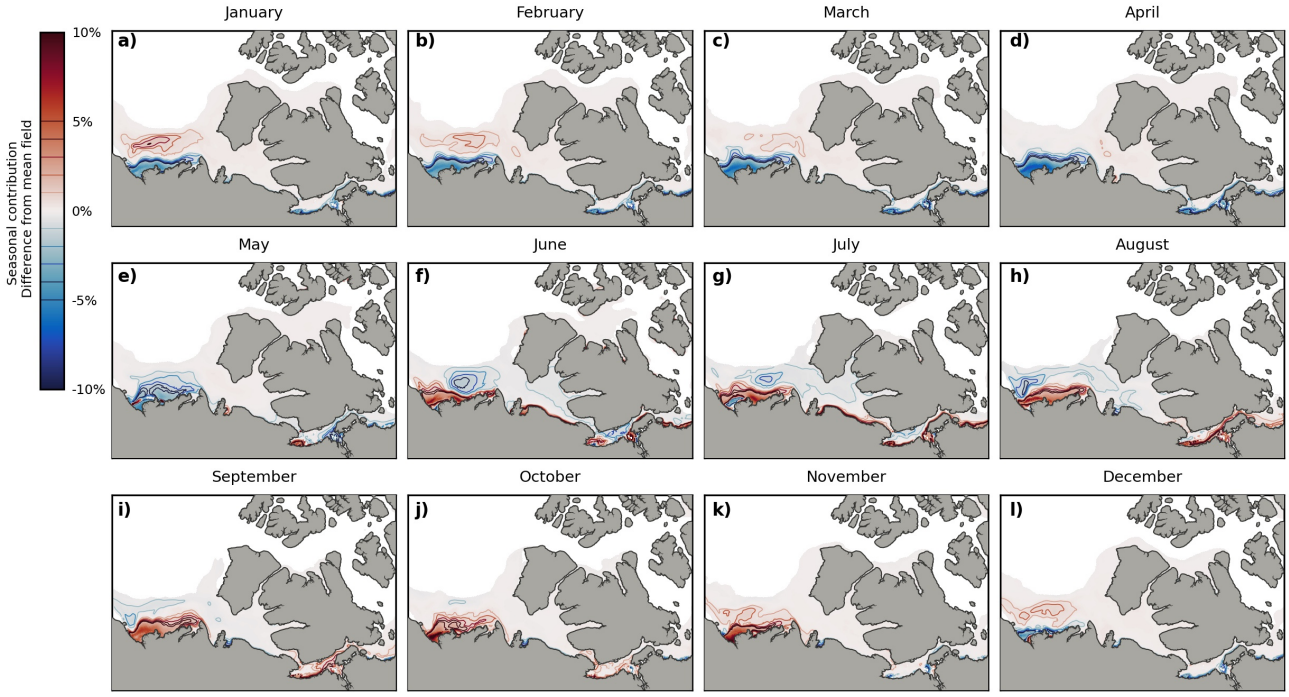

Figure S6. Monthly variations in the extent of terrestrial freshwater in the Polar Mixed Layer (upper 34 m of the water column) in the southwestern Canadian Arctic Archipelago in the "seasonality" experiment, based on climatology from 2002 to 2020. The seasonal increases (red) and decreases (blue) in contribution are calculated as a percent change from the mean field in Fig. S4

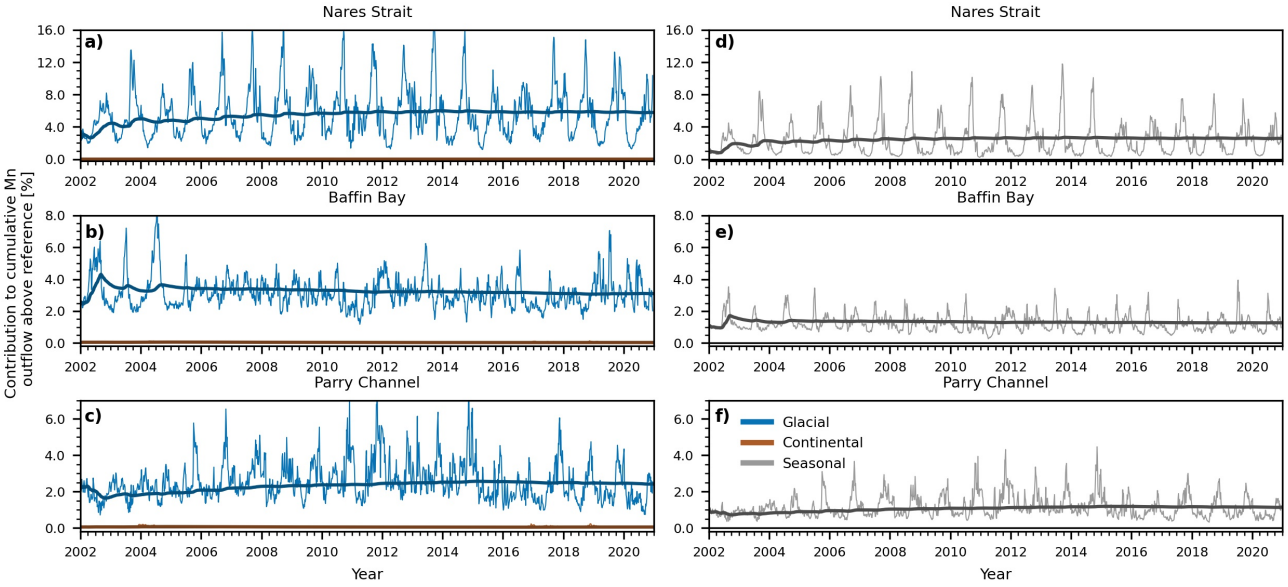

Figure S7. Time series of instantaneous (thin lines) and cumulative (thick lines) enhanced outflow (eastward and southward) along model boundaries in the "seasonality" experiment (grey, panels d-f), with the glacial melt (blue) and permafrost thaw (brown) experiments included for comparison (panels a-c). Fluxes are calculated from five-day velocity and tracer fields (Eqn. 3) and compared with the reference run (Eqn. 2). The contributed percent is scaled by a factor that incorporates the multiplier applied to the Mn runoff forcing at peak flow, so that if the Mn flux increases exactly by the additional Mn added in runoff, the contribution is 100%. The boundaries at which fluxes are calculated are shown with black dashed lines in Fig. 2a.

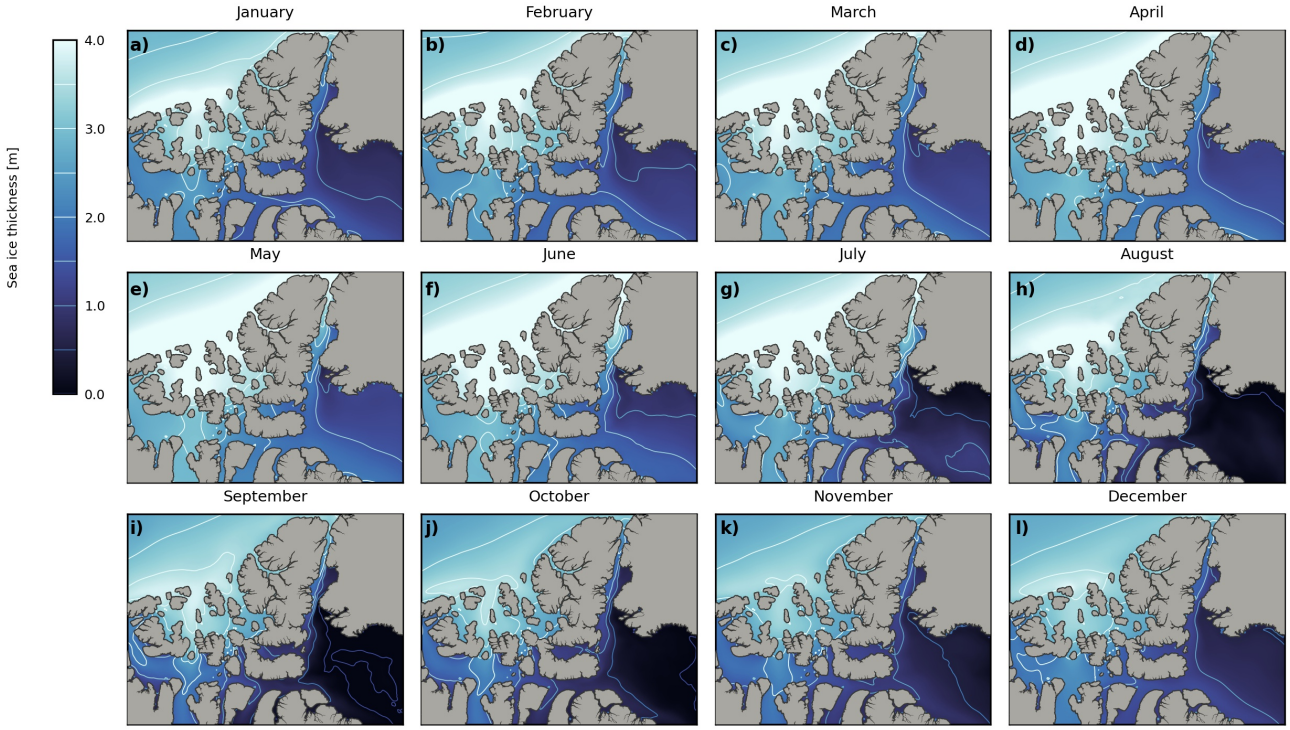

Figure S8. Monthly climatology of modelled sea ice thickness over the northeastern Canadian Arctic Archipelago, averaged over 2002 to 2020. The ANHA12 configuration of the NEMO model uses the LIM2 sea ice model.

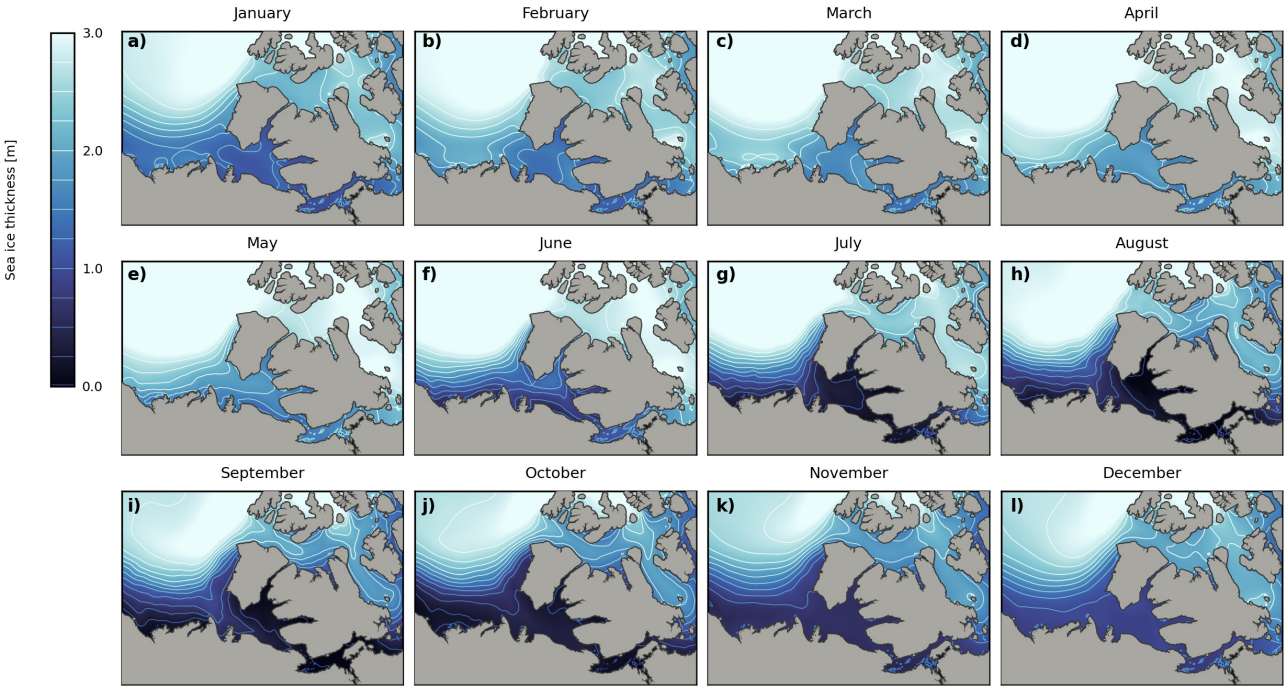

Figure S9. Monthly climatology of modelled sea ice thickness over the Beaufort Shelf and the southwestern Canadian Arctic Archipelago, averaged over 2002 to 2020. The ANHA12 configuration of the NEMO model uses the LIM2 sea ice model.

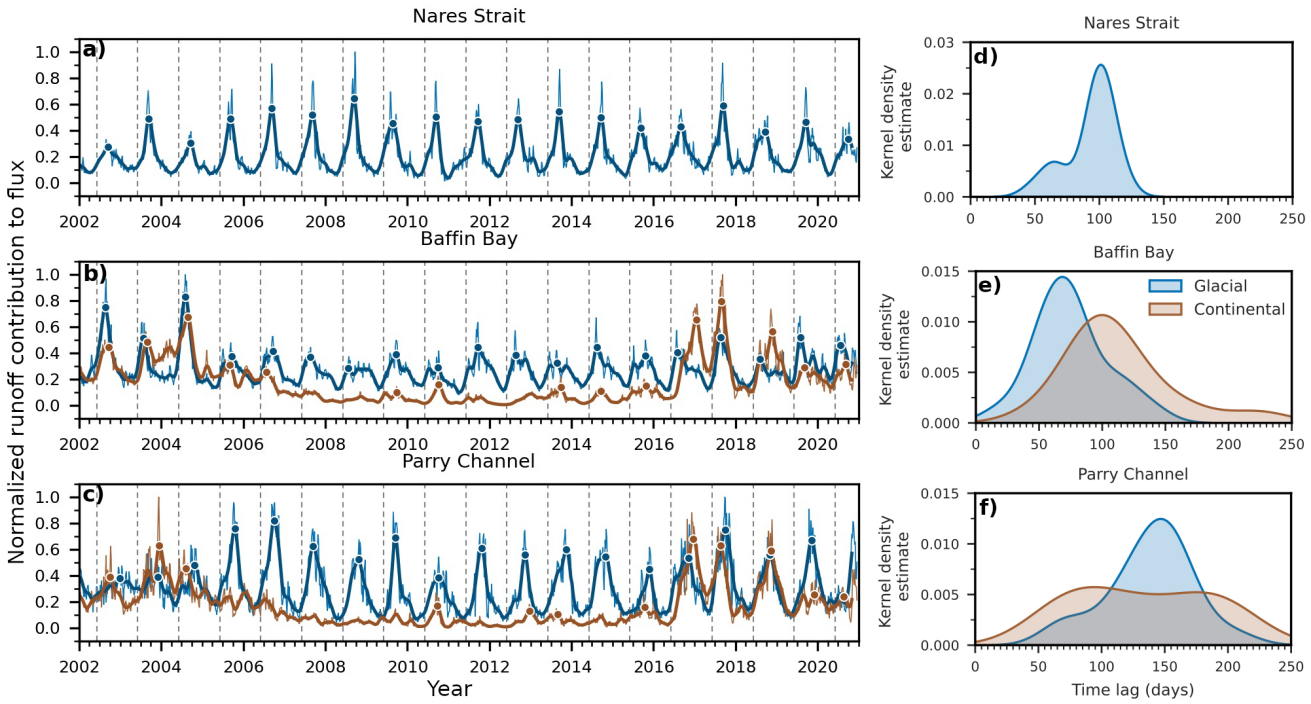

Figure S10. Runoff contributions to downstream Mn fluxes across key channels in the Canadian Arctic peak after the spring freshet. The time lag of the arrival of this maximum depends on the travel distance and route between the runoff sources and the boundaries. In panels a-c, we show the contribution of glacial (blue) and continental (brown) runoff to fluxes across each of the boundaries, normalized by their maxima during the time series. Thick lines correspond to the smoothed signal used to calculate the timing of peak runoff contribution, marked with a circle, and the peak source runoff dates are marked by the dashed gray lines. We calculated the kernel density estimates of the lag time between peak discharge and peak runoff flux at each of the (d) Nares Strait, (e) Baffin Bay, and (f) Parry Channel boundaries for the glacial and continental runoff, based on the flux time series in panels a-c.